

**Repository of the Max Delbrück Center for Molecular Medicine (MDC)
in the Helmholtz Association**

<http://edoc.mdc-berlin.de/11763>

**Genomic loss of the putative tumor suppressor gene E2A in human
lymphoma**


Steininger, A. and Moebs, M. and Ullmann, R. and Koechert, K. and Kreher, S. and Lamprecht, B. and Anagnostopoulos, I. and Hummel, M. and Richter, J. and Beyer, M. and Janz, M. and Klemke, C.D. and Stein, H. and Doerken, B. and Sterry, W. and Schrock, E. and Mathas, S. and Assaf, C.

This is a copy of the final article, which was first published online on 25 July 2011 and in final edited form in:

Journal of Experimental Medicine
2011 AUG 01 ; 208(8): 1585-1593
doi: [10.1084/jem.20101785](https://doi.org/10.1084/jem.20101785)

Publisher: [Rockefeller University Press](http://www.rupress.org)

© 2011, Steininger et al. This article is distributed under the terms of an Attribution–Noncommercial–Share Alike–No Mirror Sites license for the first six months after the publication date (see <http://www.rupress.org/terms>).

 After six months it is available under a Creative Commons License (Attribution–Noncommercial–Share Alike 3.0 Unported license, as described at <http://creativecommons.org/licenses/by-nc-sa/3.0/>).

Genomic loss of the putative tumor suppressor gene *E2A* in human lymphoma

Anne Steininger,¹ Markus Möbs,² Reinhard Ullmann,¹ Karl Köchert,⁴ Stephan Kreher,⁴ Björn Lamprecht,⁴ Ioannis Anagnostopoulos,³ Michael Hummel,³ Julia Richter,⁵ Marc Beyer,² Martin Janz,⁴ Claus-Detlev Klemke,⁶ Harald Stein,³ Bernd Dörken,⁴ Wolfram Sterry,² Evelin Schrock,⁷ Stephan Mathas,⁴ and Chalid Assaf^{2,8}

¹Max Planck Institute for Molecular Genetics, 14195 Berlin, Germany

²Department of Dermatology and Allergy, Skin Cancer Center Charité, ³Institute of Pathology, Charité-Universitätsmedizin Berlin, 10117 Berlin, Germany

⁴Hematology, Oncology and Tumorimmunology, Charité-Universitätsmedizin Berlin and Max-Delbrück-Center for Molecular Medicine, 13125 Berlin, Germany

⁵Institute of Human Genetics, Christian-Albrechts-University Kiel and University Hospital Schleswig-Holstein, Campus Kiel, 24105 Kiel, Germany

⁶Department of Dermatology, University Medical Center Mannheim, Ruprecht-Karls-University of Heidelberg, 68167 Mannheim, Germany

⁷Institute for Clinical Genetics, Dresden University of Technology, 01307 Dresden, Germany

⁸HELIOS Klinikum Krefeld, 47805 Krefeld, Germany

The transcription factor E2A is essential for lymphocyte development. In this study, we describe a recurrent *E2A* gene deletion in at least 70% of patients with Sézary syndrome (SS), a subtype of T cell lymphoma. Loss of *E2A* results in enhanced proliferation and cell cycle progression via derepression of the protooncogene *MYC* and the cell cycle regulator *CDK6*. Furthermore, by examining the gene expression profile of SS cells after restoration of *E2A* expression, we identify several *E2A*-regulated genes that interfere with oncogenic signaling pathways, including the Ras pathway. Several of these genes are down-regulated or lost in primary SS tumor cells. These data demonstrate a tumor suppressor function of *E2A* in human lymphoid cells and could help to develop new treatment strategies for human lymphomas with altered *E2A* activity.

CORRESPONDENCE

Chalid Assaf:
chalid.assaf@charite.de
OR

Stephan Mathas:
stephan.mathas@charite.de

Abbreviations used: AAD, aminoactinomycin D; CGH, comparative genomic hybridization; EMSA, electrophoretic mobility shift assay; FISH, fluorescence in situ hybridization; SS, Sézary syndrome.

E-proteins define a distinct class of basic helix-loop-helix transcription factors that are central regulators of cellular differentiation in various cell types and are essential for the development of B and T lymphocytes (Kee, 2009). There are three known E-protein coding genes in mammals, namely *E2A* (also called *TCF3*), *E2-2* (also called *TCF4*) and *HEB* (HeLa E-box binding protein; also called *TCF12*), which all bind to a DNA sequence motif called E-box (CANNTG). The *E2A* gene, which is located on chromosome 19p13.3, encodes for two different basic helix-loop-helix transcription factors, E12 and E47, which are generated by alternative splicing (Mellentin et al., 1989; Murre et al., 1989). *E2A* proteins form homodimers and heterodimers with other HLH

proteins to conduct their tissue- or cell type-specific functions (Kee, 2009).

Alterations of *E2A* expression and activity have been suggested to support malignant transformation of lymphoid cells. In mice, deletion of *E2A*, as well as enforced expression of its inhibitors, e.g., the inhibitor of DNA binding (Id) proteins, lead to rapid development of aggressive T cell lymphomas and T cell hyperproliferations (Bain et al., 1997; Yan et al., 1997; Morrow et al., 1999). In humans, diminished *E2A* activity has been proposed as a pathogenetic mechanism in TAL1/SCL- or *E2A*-PBX1-induced leukemias (Park et al., 1999; Aspland et al., 2001; O'Neil et al., 2004), and functional blockade of *E2A* is involved in

A. Steininger and M. Möbs contributed equally to this paper.
S. Mathas and C. Assaf contributed equally to this paper.

© 2011 Steininger et al. This article is distributed under the terms of an Attribution-Noncommercial-Share Alike-No Mirror Sites license for the first six months after the publication date (see <http://www.rupress.org/terms>). After six months it is available under a Creative Commons License (Attribution-Noncommercial-Share Alike 3.0 Unported license, as described at <http://creativecommons.org/licenses/by-nc-sa/3.0/>).

the pathogenesis of human lymphomas (Mathas et al., 2006, 2009; Lietz et al., 2007). However, a frequent genomic loss of *E2A* has not been identified in human lymphoid malignancies so far. Arguing for a function as tumor suppressor in human cells, our study now demonstrates a recurrent deletion of *E2A* in leukemic cells of patients suffering from Sézary syndrome (SS), an aggressive variant of primary cutaneous T cell lymphoma characterized by the presence of neoplastic T cells in skin, lymph nodes, and peripheral blood (Willemze et al., 2005).

RESULTS AND DISCUSSION

In a genome-wide analysis of peripheral blood mononuclear cells from 20 SS patients (Table S1) by array comparative genomic hybridization (array CGH), we identified a minimal common region of chromosomal loss on chromosome 19p13.3 in 70% (14/20) of patients (Fig. 1 A, Table I, Fig. S1, and Table S2). This region of ~1.4 Mb ranging from chr19:1368087 to chr19:2824434 (HG18) included the *E2A* gene locus. Fluorescence in situ hybridization (FISH) analysis on highly enriched tumor cells using an *E2A*-specific probe confirmed a heterozygous loss of *E2A* in 8/12 analyzed SS patient samples (Fig. 1 B and Table I; for details on tumor cell enrichment see Materials and methods, Fig. S2, and Table S3). The number of cases with *E2A* deletion might even be underestimated because in two cases without deletion in array CGH analysis, a deletion of *E2A* was detected by FISH (Table I). Concomitant with the genomic loss of *E2A*, the *E2A* mRNA expression level in enriched leukemic cells of SS patients was significantly reduced compared with purified CD4⁺ T cells from healthy volunteers (Fig. 1 C and Fig. S3 A; note, that the ΔCt of *E12/E47* or *E47*, respectively, is significantly lower in CD4⁺ controls compared with SS patient samples. Hence, relative to *GAPDH*, SS patient samples express less *E12/E47* or *E47* mRNA, respectively, than the control CD4⁺ T lymphocytes), and immunohistochemistry showed weak or absent *E2A* protein expression in skin-infiltrating tumor cells in 15/15 patient samples (Fig. 1 D).

Among cutaneous T cell lymphomas, SS is unique in respect to the presence of a high load of lymphoma cells in the peripheral blood. Because *E2A* interferes with cell cycle control (Park et al., 1999; Murre, 2005), we first investigated the impact of reduced *E2A* expression on the growth of malignant SS cells. To this end, we chose the SS-derived Se-Ax cell line, which is associated with a heterozygous loss of *E2A* (Fig. 1 B and Table I) and is characterized by reduced *E2A* mRNA and protein levels and impaired E-box DNA binding activity (Fig. 1, E and F and Fig. S3 B). After transient transfection with a Myc-tagged E47 construct and, alternatively, a construct coding for two covalently linked E47 molecules (E47-forced dimer, E47-FD), Se-Ax cells showed a pronounced reduction of proliferation (Fig. 2 A). No significant effect on apoptosis induction was observed (unpublished data). To prove the biological significance of our transfection approach, we investigated transgene expression as well as the resulting *E2A*-DNA binding

activity by immunoblotting and electrophoretic mobility shift assay. In both analyses, we reached levels comparable to endogenous ones in other T cell leukemia-derived cell lines (Fig. S3 C). To substantiate our finding of reduced proliferation after *E2A* reconstitution, we measured DNA synthesis (determined by BrdU incorporation) and the respective cell cycle phases (determined by 7-aminoactinomycin D [7-AAD] staining) in parallel by a two-color flow cytometric analysis (Fig. 2 B). This experimental approach revealed that reexpression of *E2A* in Se-Ax cells significantly increased the fraction of cells in the G0/G1 phase at the expense of cells in the S phase of the cell cycle, suggesting that the reduced proliferation of Se-Ax cells after *E2A* reconstitution is caused by a G0/G1 cell cycle arrest.

To establish a mechanistic link between *E2A* reduction and deregulated cell cycle control, we analyzed mRNA expression of the protooncogene *MYC* and the cell cycle regulator *CDK6* in Se-Ax cells. After *E2A* reconstitution, we observed significantly reduced mRNA levels of both genes (Fig. 2 C), suggesting a pathogenetically relevant link in these human T cell-derived lymphoma cells. In line with these *in vitro* data, we observed robust protein expression of *CDK6* in 7 out of 7 and, in accordance with previously published data (Vermeer et al., 2008), of *MYC* in 5 out of 6 primary SS tumor samples (Fig. 2 D). The high level of *MYC* expression in the SS tumor cells is in the majority of our SS cases most likely supported by genomic gains of chromosome 8q, which also includes the *MYC* locus (Fig. S1 and Table S4). Notably, the *MYC*-induced apoptotic program (Eischen et al., 1999) might be counteracted by the loss of 17p, including the tumor suppressor gene *TP53*, as demonstrated in a large number of our SS patient samples (Table S4).

To further investigate the impact of diminished *E2A* expression on SS tumor cells, we characterized *E2A*-dependent transcriptional changes in Se-Ax cells by microarray gene expression analyses. A highly overlapping, limited number of genes were responsive to *E2A* reconstitution with either E47 or E47-FD (Fig. S3 D and Table S5). Overall, far more genes were induced than repressed. Arguing for the biological relevance of our microarray analyses, the *E2A*-regulated genes in our data showed a significant overlap with *E2A*-dependent genes identified in *E2A*-deficient murine T cell lymphoma (Schwartz et al., 2006) and in a murine *E2A*-deficient hematopoietic progenitor cell line (Ikawa et al., 2006; Fig. S3 E and Table S6). In our dataset, among the *E2A*-induced genes were proapoptotic genes like *BCL2L11* and *BIK*, genes known to modulate T cell-specific signaling pathways and differentiation (*DTX1*, *MAL*), as well as negative regulators of oncogenic signaling pathways including the Ras signaling pathway (*RASSF4*, *DAB2IP*, *RASA4*, *RGS16*). The *E2A*-dependent up-regulation of these genes was confirmed by quantitative PCR (Fig. 3 A). In view of their dependency on *E2A*, expression would be expected to be down-regulated or lost in SS tumor cells because of their reduced *E2A* expression. Accordingly, *BCL2L11* and *MAL* were previously described to be specifically

down-regulated in SS cells (Kari et al., 2003; van Doorn et al., 2004). In our samples, *BCL2L11*, *DTX1*, and *RASSF4* were found to be down-regulated in 4/4 of our SS patient

samples, whereas reduced levels of *RGS16* were observed in 2/4 SS samples compared with normal CD4⁺ T cells (Fig. 3, B and C).

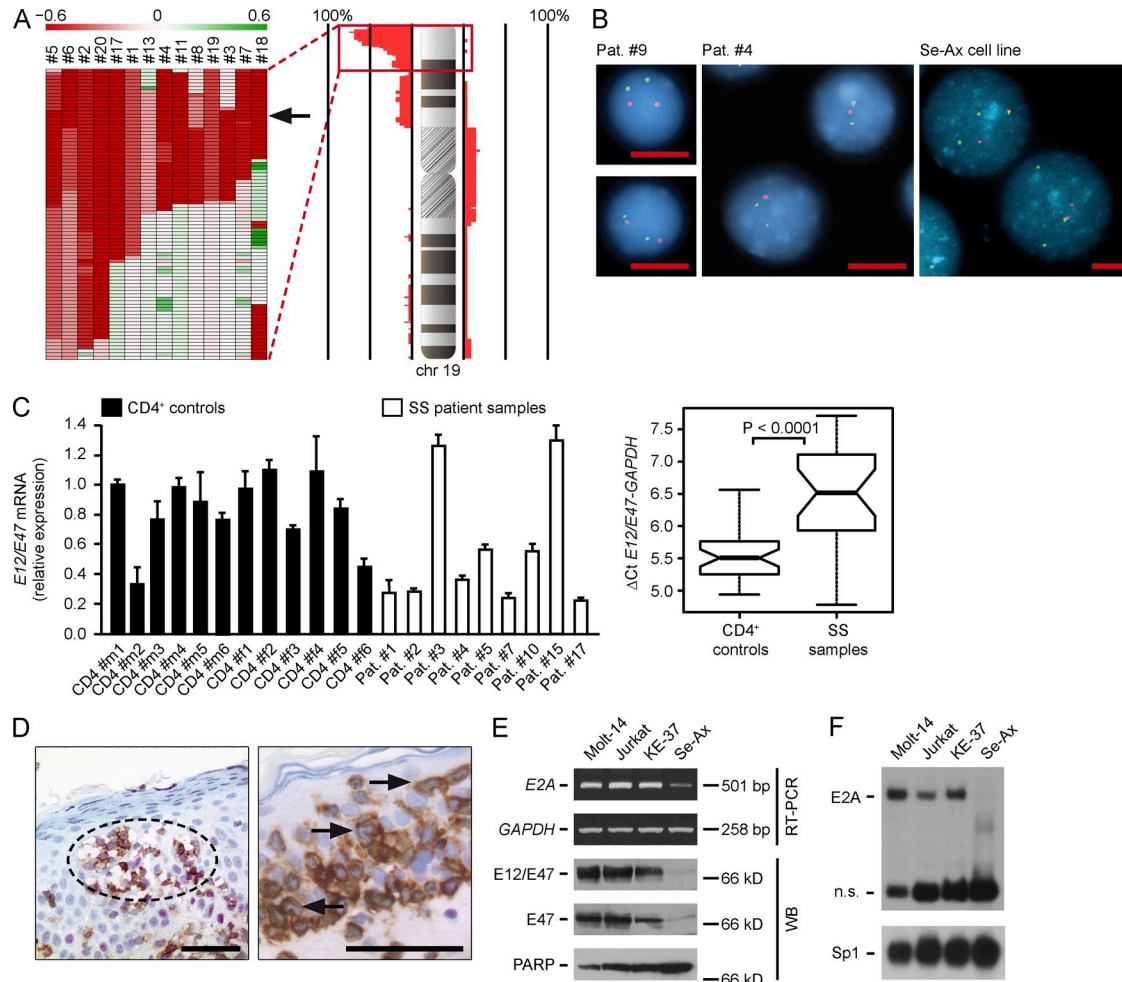


Figure 1. Loss of *E2A* is a common feature in SS tumor cells. (A) Array CGH results for chromosome 19 in tumor cells of 14 SS patients. The frequency of chromosomal gains and losses in percent of studied cases is shown to the right and to the left of the chromosome ideogram, respectively. The genomic interval ranging from chr19: 200000–8599999 (HG18) is enlarged in the adjacent heatmap to the left. The coloring of each box in this heatmap represents the average array CGH ratio based on a 100-kb window for those 14 cases harboring *E2A* deletions according to CGH results. Chromosomal deletions and gains are shown in red and green, respectively (maximal color saturation at a log₂ ratio of 0.6/–0.6). The arrow indicates the genomic position of *E2A*. (B) Dual-color FISH analyses of purified tumor cells (patients #9 and #4) and the SS-derived cell line Se-Ax. Cells were hybridized with an *E2A* probe (red) and a control probe on 19qter (green). Pictures show representative examples of tumor cells without *E2A* deletion (Pat. #9: two red signals/two green signals) and cells with heterozygous deletion of the gene locus (Pat. #4, one red/two green; Se-Ax cells, two red/three green signals). Bars, 5 μm. (C) Quantification of *E2A* mRNA levels by real-time PCR in CD4⁺ T lymphocytes from healthy volunteers and purified leukemic SS cells from various patients, as indicated. (left) *E2A* mRNA expression in the various samples was analyzed relative to *GAPDH* by quantitative real-time PCR using primers recognizing both *E2A* splice variants, *E12* and *E47*. (right) Box plot presentation of the comparison of ΔCt values of *E2A* in CD4⁺ controls (six male [CD4 #m] and six female [CD4 #f] samples) and SS patient samples (Pat. #). Results are shown for one of two independent experiments performed. (D) Immunohistochemistry of SS skin biopsies. Shown is double staining of the T cell marker CD3 (brown) and *E12/E47* (purple). Dashed circle designates accumulations of malignant lymphocytes in the epidermis, so called Pautrier's microabscesses. Arrows point to individual tumor cells with cerebriform nuclei. Bars, 50 μm. (E and F) *E2A* expression and DNA binding activity in various cell lines. (E, top) RT-PCR analysis of *E2A* mRNA expression in T cell-derived control cell lines Molt-14, Jurkat, and KE-37, as well as SS-derived Se-Ax cells. (bottom) Analysis of *E2A* protein expression in nuclear extracts of various cell lines by Western blotting (WB) using antibodies to both *E2A* splice variants *E12* and *E47* (*E12/E47*) or to *E47*. *GAPDH* and *PARP* were analyzed as controls. Results are shown for one of three independent experiments performed. (F) EMSA of *E2A* DNA-binding activity in the various cell lines, as indicated. Sp1 DNA binding was analyzed as a control. Positions of the specific protein–DNA complexes are indicated. n.s., nonspecific complex. Results are shown for one of three independent experiments performed.

Apart from their central role in B and T lymphocyte development, E2A proteins have been suggested to act as tumor suppressors (Bain et al., 1997; Yan et al., 1997). Although other genes located at 19p13.3 might also contribute to the pathogenesis of SS, our data identify the loss of *E2A* as a pathogenetically important defect of SS tumor cells and strongly support a role of *E2A* as a tumor suppressor in human lymphoid cells. Mechanistically, we provide evidence that E2A controls a whole set of genes known to promote tumorigenesis. Concomitant with an increased proliferation rate, most likely caused by an impaired G0/G1 cell cycle checkpoint, loss of *E2A* resulted in an up-regulation of *MYC* and *CDK6*. Both genes have been described as E2A target genes in lymphomas that emerge in *E2A*-deficient mice (Schwartz et al., 2006) and are known to be involved in lymphocyte proliferation, survival, and differentiation (Herold et al., 2009; Hu et al., 2009). Furthermore, aggressive T cell lymphomas in *E2A*-deficient mice are characterized by high-level *myc* expression (Bain et al., 1997). This suggests that up-regulation of the *MYC* oncogene is a common phenomenon after loss of E2A, most

likely by loss of transcriptional repression. Speculations on the interconnection of *MYC*, *E2A*, and *TP53* and their synergistic influence on lymphoma development are substantiated by the high number of cases with simultaneous DNA copy number changes affecting these genes in our SS samples, as well as in *E2A*-deficient lymphoma cells in mice, a fact that most likely reflects the selective advantage provided by the combination of these aberrations (Fig. S1 and Table S4; Bain et al., 1997). Up-regulation of *CDK6* as a consequence of reduced E2A levels could represent another strategy of SS cells to provide a growth and survival advantage. Higher levels of *CDK6* in SS cells might cooperate with an aberrant activation of the NOTCH signaling pathway, because *CDK6* is necessary to exert the proliferative and anti-apoptotic function of NOTCH (Hu et al., 2009). NOTCH itself promotes T lymphomagenesis (Koch and Radtke, 2007) and is required for the survival of *E2A*-deficient lymphoma cells in mice (Reschly et al., 2006). In line with this concept, NOTCH activation has been reported in SS cells (Kamstrup et al., 2010). In addition, our data show that E2A controls negative regulators of the oncogenic

Table I. Loss of *E2A* in SS tumor cells

Patient no.	Loss of <i>E2A</i>		Purity of enriched tumor cells
	Array CGH analysis	FISH analysis (number of cells with deletion/number of analyzed cells)	
			%
1	yes ^c	yes (149/200) ^e	96.7
2	yes ^c	n.d.	-
3	yes ^c	yes (198/200) ^e	99.1
4 ^a	yes ^c	yes (167/200) ^e	93.2
5	yes ^e	yes (90/200) ^e	97.9
6	yes ^d	n.d.	-
7 ^a	yes ^c	no (14/200) ^e	99.2 ^f
8	yes ^e	n.d.	-
9	no ^c	no (3/200) ^e	97.4
10	no ^c	no (4/200) ^e	96.9
11 ^a	yes ^e	no (12/200) ^d	n.d.
12	no ^c	n.d.	-
13	yes ^c	yes (126/200) ^e	98.4 ^f
14	no ^c	n.d.	-
15 ^a	no ^{b,c}	yes (106/200) ^d	n.d.
16 ^a	no ^e	yes (loss 28/200, gain 46/200) ^e	97.2
17	yes ^e	yes (50/200) ^e	98.4
18	yes ^c	n.d.	-
19	yes ^e	n.d.	-
20	yes ^e	n.d.	-
Se-Ax cell line	yes	yes (190/200)	

n.d.: not determined

^aCGH and FISH analyses were performed with samples from different time points (see Table S1).

^bhypotriploid cells, gain of chromosome 19 except 19p13.2-13.3.

^cAnalysis of PBMC cells.

^dAnalysis of CD4-sorted cells.

^eAnalysis of Vβ-sorted cells.

^fPurity was determined with CD4 antibody only.

Ras signaling pathway (*RASSF4*, *RASA4*, and *DAB2IP*). Although altered expression of each of these genes alone might result in Ras activation (Eckfeld et al., 2004; Lockyer et al., 2001; Min et al., 2010), activation of the Ras signaling pathway has still to be proven formally in SS cells. Therefore, the therapeutic potential of Ras inhibition in lymphomas with reduced E2A activity has to be investigated in future studies.

By FISH analysis, no homozygous deletion of *E2A* was observed. Direct sequencing of the coding regions of all *E2A* exons in leukemic SS cells from 13 patients did not reveal deleterious mutations or deletions (Table S7). Furthermore, the investigated *E2A* promoter regions in enriched SS cells compared with normal CD4⁺ T cells did not show altered methylation patterns Fig. S4. These data suggest on the one hand that the reduction of E2A expression after monoallelic *E2A* deletion might be sufficient for lymphoma progression, and on the other hand that selective pressure exists to retain one *E2A* copy to ensure a certain level of E protein activity, which is probably necessary for cellular survival at some time point during lymphomagenesis. Lowering the

E2A dosage might facilitate the posttranslational degradation of E2A by NOTCH1 (Nie et al., 2003), which is aberrantly activated in SS cells (Kamstrup et al., 2010). Such a model, i.e., that lowering of wild-type E2A expression contributes to human lymphomagenesis, is supported by the finding of aberrant up-regulation of E2A antagonists like inhibitory HLH proteins (O'Neil et al., 2004; Lietz et al., 2007; Mathas et al., 2006, 2009) or the disruption of one *E2A* allele and maintenance of one wild-type allele as a result of translocations involving the *E2A* locus (Aspland et al., 2001) in human lymphoma cells. That even a subtle dosage reduction of a putative tumor suppressor is sufficient for tumor formation has recently been formally shown for, e.g., PTEN (Alimonti et al., 2010).

Together, our data highlight the genomic loss of 19p13.3 including the *E2A* locus as a pathogenetically important defect of human T cell-derived SS lymphoma cells. Our results provide insights into how E2A acts as a tumor suppressor in human lymphoid cells and might help to develop new treatment strategies for human lymphomas with lost or reduced E2A activity.

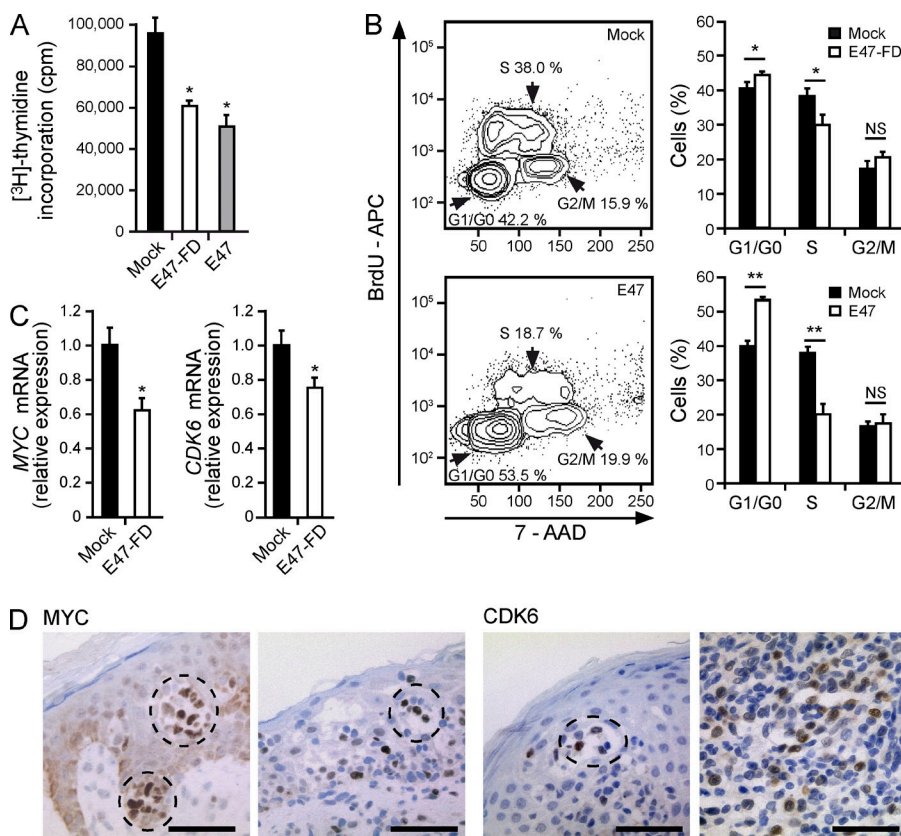


Figure 2. E2A-dependent proliferation and expression of MYC and CDK6 in SS cells.

(A) Reconstitution of E2A expression in SS-derived Se-Ax cells. Se-Ax cells were transfected with Mock plasmid (control) or plasmids encoding Myc-tagged E47 (E47) or E47-FD, as indicated, along with pEGFP. EGFP⁺ cells were purified 48 h after transfection, pulsed with 1 μ Ci [³H]thymidine per well for another 20 h, and then [³H]thymidine incorporation was determined. Error bars denote standard deviation. Results are shown for one of three independent experiments performed. *, $P < 0.001$. (B) Proliferation and cell cycle analyses of Se-Ax cells after E2A reconstitution. Se-Ax cells were transfected as described in A. 48 h after transfection, cells were pulsed for 30 min with BrdU. Thereafter, transfected cells were gated based on their EGFP expression, and BrdU incorporation and 7-AAD staining was measured by flow cytometry in GFP⁺ cells. Left, representative examples for detection of BrdU incorporation and 7-AAD staining by flow cytometry in Mock- (top) or E47- (bottom) transfected Se-Ax cells. Positions and percentages of cells in cell cycle phases G0/G1, S, and G2/M are indicated. Right, summary of cell cycle analyses of Mock- vs. E47-FD- (top) and E47- (bottom) transfected Se-Ax cells. The fraction of cells in the respective cell cycle phases is indicated in percent. Error

bars denote standard deviations. Results are shown for one of three independent experiments performed. *, $P < 0.05$; **, $P < 0.005$; NS, not significant. (C) Se-Ax cells were transfected with E47-FD and purified as described in A. Expression of *MYC* and *CDK6* mRNA was assessed by quantitative PCR. Error bars denote 95% confidence intervals. Results are shown for one of three independent experiments performed. *, $P < 0.001$. (D) Representative *MYC* and *CDK6* immunohistochemistry of each two SS skin biopsies. *MYC* and *CDK6* stainings are in brown. Dashed circles designate Pautrier's microabscesses. *CDK6*, right, *CDK6* expression in cells with frequent cerebriform nuclei within a dermal infiltrate from a patient with SS. Bars, 50 μ m.

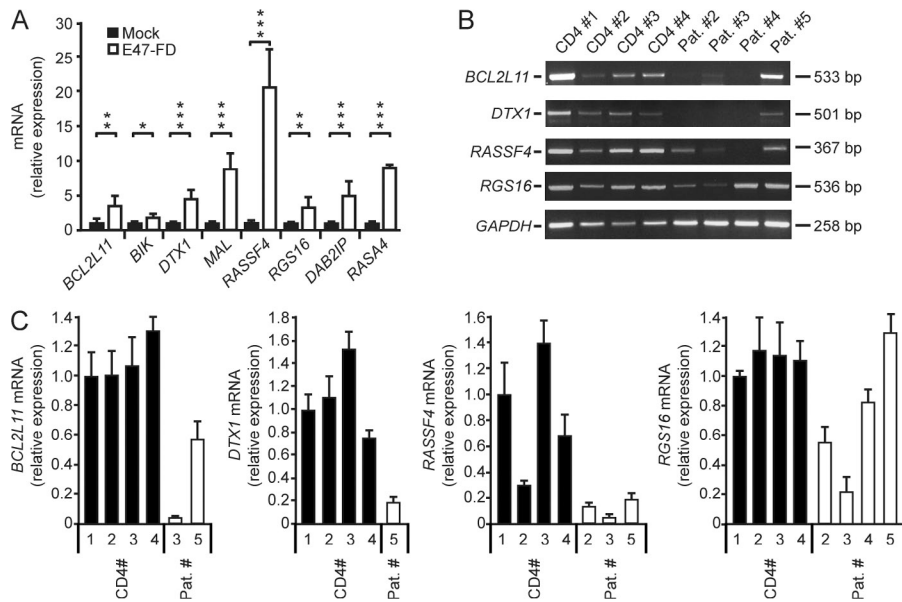


Figure 3. E2A-regulated genes in SS tumor cells. (A) Se-Ax cells were transfected with Mock plasmids (control) or plasmids encoding E47-FD, along with pEGFP. 48 h after transfection, EGFP⁺ cells were enriched. Expression of various genes, as indicated, was assessed by quantitative PCR. Error bars denote 95% confidence intervals. Results are shown for one of four independent experiments performed. *, $P < 0.5$; **, $P < 0.01$; ***, $P < 0.001$. (B and C) mRNA expression of various genes in purified CD4⁺ T cells from healthy donors (CD4 #1 to CD4 #4) compared with enriched tumor cells derived from four SS patients (Pat. #2, #3, #4, #5; numbers refer to the same patients listed in Table I). If mRNA expression was detectable in SS samples by semiquantitative PCR (B), mRNA expression was quantified by real-time PCR in the respective samples (C). Error bars denote 95% confidence intervals. Results are shown for one of two independent experiments performed.

MATERIALS AND METHODS

Patient samples. 20 clinically well-characterized patients with SS were included in our study. Diagnoses were established according to the World Health Organization-European Organization for Research and Treatment of Cancer classification for cutaneous lymphomas (Willemze et al., 2005). Detailed clinical information on all patients and blood samples are summarized in Table S1. The use of human material was approved by the Local Ethics Committee of the Charité-Universitätsmedizin Berlin and performed in accordance with the Declaration of Helsinki.

Clonality analysis and sequencing of tumor cell-specific TCR β rearrangements. PBMC samples were analyzed for the presence of a clonally expanded tumor cell population by TCR β -rearrangement PCR analysis using primers and protocols developed within the BIOMED-2 BMH4-CT98-3936 Concerted Action initiative (van Dongen et al., 2003). Only samples that showed almost single clonal product peaks in the fluorescent fragment analysis (FFA) were directly used for subsequent CGH analysis. To identify the V β chain expressed by the respective tumor cells, amplification products were purified and complete TCR β rearrangements were sequenced using the BigDye Terminator V1.1 cycle sequencing kit (Applied Biosystems) and subsequent analysis by high resolution electrophoresis on an ABI PRISM 310 Genetic Analyzer. Identification of the involved V, D, and J segments was done by submitting the received TCR β sequence to the International Immunogenetics Information System V-QUEST tool (http://imgt.cines.fr/IMGT_vquest/share/textes/; Brochet et al., 2008; Lefranc et al., 2009). Results for each patient are presented in Table S3.

Enrichment of primary SS tumor cells from PBMCs. PBMCs were isolated from whole blood or leukapheresis samples by density gradient centrifugation using Ficoll-Paque-Plus (GE Healthcare). For enrichment of tumor cells, PBMCs were incubated for 30 min with the respective fluorochrome-conjugated V β antibody (Beckman Coulter; see Table S3 for details) at a concentration of 5–20 μ l/ 10^6 cells in 100 μ l of MACS buffer, followed by incubation with anti-fluorochrome MicroBeads (Miltenyi Biotec). Cells were magnetically separated by use of LS columns (Miltenyi Biotec) according to the manufacturer's recommendations. Where indicated, tumor cells were enriched after incubation with anti-CD4 microbeads (Miltenyi Biotec). The purity of enriched cells was determined by flow cytometry.

Flow cytometric analysis of tumor cell samples. PBMCs and enriched tumor cells were analyzed on a FACSCalibur flow cytometer (BD) using CellQuest Pro software (BD) and WinMDI version 2.9 (The Scripps Research Institute). Antibodies directed against CD3, CD4, and CD8 were purchased from BD. All V β -chain specific antibodies were from Beckman Coulter (see Table S3 for details).

Cell lines, culture conditions, proliferation, and cell cycle analysis. The human SS-derived cell line Se-Ax (Kaltof et al., 1987); the T cell acute lymphoblastic leukemia (T-ALL) cell lines Molt-14, Jurkat, and KE-37; and H9 cells were cultured as previously described (Mathas et al., 2009), apart from adding 100 U/ml recombinant human IL-2 (Sigma-Aldrich) to Se-Ax cell culture medium. Se-Ax cells were electroporated in OPTIMEM I (Invitrogen) using a Gene-Pulser II (Bio-Rad Laboratories) with 500 μ F and 0.24 kV. Transfection efficiency was determined by pEGFP-N3 (Takara Bio Inc.) co-transfection and subsequent flow cytometry. Cells were transfected with 30 μ g myc-tagged E47 or E47-FD expression constructs (Sigvardsson et al., 1997; Lietz et al., 2007) or 30 μ g control plasmid pCDNA3.1 (Invitrogen), along with 10 μ g of pEGFP-N3. 48–72 h after transfection, EGFP⁺ cells were enriched by FACS sorting, and sorted cells were used for proliferation assays as well as RNA and protein preparation. Proliferation of cells was determined by measurement of DNA synthesis after [³H]thymidine incorporation using standard protocols. Parallel measurement of BrdU incorporation for determination of proliferation and of 7-AAD staining for determination of cell cycle position was performed by use of the APC BrdU Flow kit (BD). In brief, 48 h after transfection, cells were pulsed for 30 min with BrdU, and BrdU incorporation and 7-AAD staining in gated EGFP⁺ cells was determined by flow cytometry.

Array CGH. Initial array CGH analysis was done by means of a submegabase resolution BAC array, as described previously (Erdogan et al., 2006). DNA copy number changes were defined by circular binary segmentation (Olshen et al., 2004) in combination with a \log_2 threshold of 0.2/–0.2. Aberrations encompassing chromosome arm 19p were further verified and fine-mapped by hybridizations onto a 400k whole genome (Agilent; Gene Expression Omnibus [GEO] accession no. GPL9777) and a customized 60k chromosome 19p oligonucleotide array (Agilent; GEO accession no. GPL10304), respectively, following the manufacturer's recommendations (Table S8). The customized array comprised 52,828 oligonucleotides evenly covering chromosomal region chr19: 1–28,500,000 (NCBI36; HG18). Array CGH data discussed in this work are available (Barrett and Edgar, 2006) under GEO accession no. GSE19000.

FISH analysis of *E2A*. FISH analysis was performed on enriched tumor cells using the specific DNA-probes spanning the *E2A* gene (RP11-690N6) and control probes for 19qter (D19S989; Kretech) to judge the copy number of chromosome 19. Hybridization, detection, dual color image acquisition, and image analysis were performed as previously described (Schröck and Padilla-Nash, 2000).

RNA preparation, semiquantitative, and real-time PCR analyses. Total RNA was prepared using the RNeasy kit (QIAGEN). First strand cDNA-synthesis was performed by use of the first-strand cDNA synthesis kit (AMV; Roche) adding oligo-p(dT)15 primer according to the manufacturer's recommendation. For semiquantitative PCR analyses primers were as follows: *GAPDH*, sense (s) 5'-ATGCTGGCGCTGAGTAC-3' and antisense (as) 5'-TGAGTCCTCCACGATAC-3'; *E2A*, s 5'-CACCTCCCTGACCTGTCT-3' and as 5'-GGAGCTGAAAGCACATCTG-3'; *RGS16*, s 5'-TGGAGAGAGTCGTTTCGACCTG-3' and as 5'-TGTCTCTTGCACCTGCTTTGC-3'; *RASSF4*, s 5'-GGTGGGATGACTTCAATG-3' and as 5'-GTGGCTTCCAAGCTATGCTC-3'; *BCL2L11* s 5'-GGGTGACTGGAGAGCTCATT-3' and as 5'-AAAGCAGGAAGTTGCACA-3'; *DTX1*, s 5'-CTGGTCACAGCATCAGCTA-3' and as 5'-GGTCTTGTGGTGGATCTCGT-3'. Real-time PCR analyses were performed using Power SYBR Green Mastermix and the ABI StepOnePlus real-time PCR system (Applied Biosystems). Three technical replicates were performed for each reaction and specificity of PCR products was confirmed by melting curve analysis and subsequent agarose gel electrophoresis. Relative expression values were determined using the 2^{-ΔΔCt} method. Calculations were done with the StepOnePlus software, taking into account the determined primer efficiency of each primer set used. Primers used for real-time PCR analyses were as follows: *myc*, s 5'-TCAAGAGGTGCCACGTCTCC-3' and as 5'-TCTTGGCAGCAGGATAGTCCTT-3'; *CDK6*, s 5'-GGCTGTGTGAACCAGCCCAAG-3' and as 5'-TGGCCAGCCTAGACAGGCA-3'; *DTX1*, s 5'-TCAGGCTACGAGGGCGTCT-3' and as 5'-CCACGAGGCACAGGTGG-3'; *BIK*, s 5'-AGCTCCTGGAACCCCCGACC-3' and as 5'-CGCAGGGCCAATGCGTCACT-3'; *MAL*, s 5'-GGTGGGAAGTGGCAGCCGTG-3' and as 5'-ACAAGATGGGGCGCTCGGGA-3'; *RASSF4*, s 5'-TTGGGCGTGAAGTCCCCCA-3' and as 5'-AGGCGCTGCAGCATCGTCAG-3'; *BCL2L11*, s 5'-TGCCAGCCCTGGCCCTTTTG-3' and as 5'-GGCCTGGCAAGGAGACTTGG-3'; *RGS16*, s 5'-TCAGCCGCCTTGCCACTCT-3' and as 5'-CGGCTGGCTTCCTCACTGCC-3'; *RASA4*, s 5'-TTTGGCGGCTCGCACGTCAT-3' and as 5'-CACCTCCGACGCGCAGACA-3'; *DAB2IP*, s 5'-CTGTGTG-CAGCCCTCGAGCC-3' and as 5'-GAGGTGCTCGTTGCCCCGC-3'; *TBP*, s 5'-CAGGACCAAGAGTGAAGAACA-3' and as 5'-AGCTGAAAAACCAACTTCTGT-3'; *GAPDH*, s 5'-CTCTGCTCCTCCTGTTTCGAC-3' and as 5'-TTAAAAGCAGCCCTGGTGAC-3'; TaqMan Gene Expression Assays Hs01012686_m1 (*E47*), Hs0102692_g1 (*E12/E47*), and Hs03929097_g1 (*GAPDH*). For statistical analyses, independent Student's *t* tests were used. All PCR products were verified by sequencing.

Direct sequencing of *E2A* coding regions. All 18 coding exons of *E2A* (*E12* and *E47*) were amplified from 10–20 ng of genomic DNA isolated from enriched tumor cells using AccuPrime GC-Rich Polymerase (Invitrogen) according to the manufacturer's recommendations. PCR products were directly sequenced by using the BigDye Terminator V1.1 cycle sequencing kit (Applied Biosystems) and subsequent analysis on an ABI PRISM 310 Genetic Analyzer. Primer sequences for amplification and sequencing were as follows: Exon 1, s 5'-CCTCCCTGTTTCTCCCTGTC-3' and as 5'-GAA-AACCTCCCGTGAAGT-3'; Exon 2, s 5'-TGTAAGGTTTGGTTTGCCAC-3' and as 5'-CACTGCTTCAACAGACCCTTG-3'; Exon 3, s 5'-AGGTTTGCCCTGAGATGAT-3' and 3 as 5'-CAGGACTCA-AACCCATGTCC-3'; Exon 4, s 5'-GGACATGGGTTTGAGT-CCTG-3' and as 5'-GTGAACGCTGGGGACTTG-3'; Exon 5, s 5'-CCCTCAGGATGTTCTTGGG-3' and as 5'-GAGAGGTTGGGTGACAGATTG-3'; Exon 6, s 5'-AACAGCCTGGGGTCTGGATG-3'

and as 5'-CCTACCTCCCTTGCAGGCT-3'; Exon 7, s 5'-GCA-GGGGTTGTTCTCATGGC-3' and as 5'-AAGCTTCGCCAGGA-CACAGG-3'; Exon 8, s 5'-GAAACGGGGTGGTAGATGTG-3' and as 5'-GAGGGGAGCTGGTAAGGTG-3'; Exon 9, s 5'-CTATCCC-GCCCCCTTCTAC-3' and as 5'-GTTACCTCTGCTCCATGC-3'; Exon 10, s 5'-GCACGAGCGTATGGTAGGAC-3' and as 5'-CTCT-CAGGGCCAGCAGAC-3'; Exon 11+12, s 5'-CTGTGCAGGACG-GCAGAAC-3' and as 5'-CCGCAAAGCCTTCACAGA-3'; Exon 13, s 5'-ATCAGGCCATGCTCACACCC-3' and as 5'-TCTGTCTG-CAAAATCTGTCTCGG-3'; Exon 14, s 5'-CATGCGGAAGGGACATGA-3' and as 5'-GGTGGCTGCCTCCAACCT-3'; Exon 15, s 5'-GCTGGCCT-CAGGTTTTCAC-3' and as 5'-ACCCTGACCCCCACACTA-3'; Exon 16a, s 5'-CCAAGACCTGGTTTTTCCAG-3' and as 5'-GAGGGAGA-CAGTGAGGTTGG-3'; Exon 16b, s 5'-ACCCACACTGGGAGGCCGT-3' and as 5'-CAGTCATGGCAATGCGGTCA-3'; Exon 17, s 5'-TACC-CTCTCCACAACCCAGC-3' and as 5'-AGCATCTGCACCTGGG-TGTG-3'; Exon 18, s 5'-ACATCTTCTCCTCCCTGGG-3' and as 5'-GTGTGGATGTGGATGAAGCC-3'.

Bisulfite pyrosequencing. Bisulfite pyrosequencing of two amplicons located in the *E2A* promoter region was performed according to Lamprecht et al., 2010 with few modifications. In brief, genomic DNA was bisulfite converted using the EpiTect Bisulfite Conversion kit (QIAGEN). In a post-PCR amplification, locus-specific primers were used with one primer biotinylated at the 5' end (PCR and sequencing primer sequences and analyzed region are shown in the following paragraph). For *E2A* amplification reactions, PyroMark PCR kit (QIAGEN) was used according to standard protocols. After initial denaturation (95°C for 15 min), PCR consisted of 45 cycles of 94°C for 30 s, annealing temperature for 30 s, and 72°C for 30 s, followed by a final synthesis at 72°C for 10 min. Pyrosequencing was performed using the Pyrosequencer ID and the DNA methylation analysis software Pyro Q-CpG 1.0.9 (Biotage), which was also used to evaluate the ratio T:C (mC:C) at the CpG sites analyzed. All assays were optimized and validated using commercially available completely methylated DNA (Millipore) and pooled DNA isolated from peripheral blood of 10 healthy male and female controls, respectively.

Primer sequences and conditions used for bisulfite-pyrosequencing were as follows: *E2A_promA*, s 5'-TTAGTTTATGGAGGGTAGGTA-3' (5' modification, biotin) and as 5'-AAACCCCAACAATATTCA-3' (annealing temperature, 55°C; amplicon length, 126 bp; analyzed region [ucsc, HG18], chr19:1,601,941-1,602,066); *E2A_promA_seq*, s 5'-CCCTA-AATTACTTTACTAT-3'; *E2A_promB*, s 5'-TAAGGGGAAATTG-AGGT-3' and as 5'-CCCTAATACTAAACCCTACATACAA-3' (5' modification, biotin; annealing temperature, 55°C; amplicon length, 139 bp; analyzed region [ucsc, HG18], chr19:1,596,870-1,597,008); *E2A_promB_seq*, s 5'-ATTGAGGTTTTGGAG-3'.

Electrophoretic mobility shift assay (EMSA) and immunoblotting.

Preparation of whole-cell and nuclear extracts, as well as EMSA, was performed as previously described (Mathas et al., 2006). The following double-stranded oligonucleotides were used for EMSA: *E2A* (μE5) sense 5'-AGCTCCAGAA-CACCTGCAGCAG-3' and *E2A* (μE5) antisense, 5'-AGCTCTGTGCA-GGTGTTCTGG-3'; Sp1 sense, 5'-AGCTATTCGATCGGGCGGGCG-AGC-3' and Sp1 antisense, 5'-AGCTGCTCGCCCGCCCCGATC-GAAT-3'. After annealing, oligonucleotides were end-labeled with [α-³²P]dCTP using Klenow fragment. Positions of protein-DNA complexes were visualized by autoradiography. For supershift analyses, mouse monoclonal antibody to *E12/E47* (clone G98-271; BD) was used. For immunoblot analyses, the following primary antibodies were used: mouse monoclonal antibody to *E12/E47* (clone G98-271; BD), mouse monoclonal antibody to *E47* (clone G127-32; BD), goat polyclonal antibody to PARP-1 (sc-1561; Santa Cruz Biotechnology, Inc.), and mouse monoclonal antibody to β-actin (A5316; Sigma-Aldrich). Filters were incubated with horseradish peroxidase-conjugated secondary antibodies. Bands were visualized with the enhanced chemiluminescence system (GE Healthcare).

Immunohistochemistry. Immunohistochemistry was performed on 4- μ m sections obtained from formalin-fixed and paraffin-embedded material, and done according to Mathas et al., 2009. The primary antibodies used for evaluation of various proteins were monoclonal antibody to E12/E47 (clone G98-271; BD), CDK6 (clone DCS-83; Progen Biotechnik), myc (clone Y69; Epitomics), and CD3 (clone LN10; Novocastra Laboratories).

Gene expression analysis. One-color microarray-based gene expression analysis was performed following the Quick Amp Labeling protocol from Agilent (G4140-90040v5.7; Agilent). In brief, 500 ng of total RNA was reverse transcribed, and the cDNAs were used as a template for cRNA synthesis and Cy3 labeling by in vitro transcription. Hybridization was performed on whole human genome 4 \times 44k microarrays (G4112F; Agilent; GEO accession no. GPL6480). After washing, slides were scanned using an Agilent DNA Microarray Scanner G2565BA with the following settings: scan region, 61 \times 21.6 mm; scan resolution, 5 μ m; extended dynamic range, selected; TIFF, 16 bit; dye channel, green (with Green PMT XDR Hi 100% and Green PMT XDR Lo 10%). The resulting TIFF images were processed with Agilent Feature Extraction Software v10.5.1.1 using the GE1_105_Dec08 protocol. Gene expression data discussed in this work (Barrett and Edgar, 2006) are available under GEO accession no. GSE21730.

Statistical analyses. All statistical analyses were done in R v2.9.1 (<http://www.r-project.org/>). Independent, one-tailed Student's *t* test was used to analyze data from real-time PCR experiments. For analyses of proliferation assays, one-way analysis of variance was done before applying Tukey's Honestly Significant Difference test with 95% family-wise confidence level. Two-sided Welch's *t* test was applied to determine significance of cell cycle phase differences between Mock- and E47-FD- or E47-transfected cells, respectively.

Online supplemental material. In Fig. S1, the complete copy number changes detected by array CGH analysis of all analyzed patients are depicted. Fig. S2 shows a clonality analysis of a leukemic SS patient before and after tumor cell enrichment. Fig. S3 shows *E47* mRNA expression levels in SS patient samples. Fig. S4 shows methylation of two regions within the promoter region of *E2A* in SS patient samples compared with purified CD4⁺ T lymphocytes from healthy volunteers. Table S1 shows detailed information on SS patient samples. Table S2 shows the exact positions of the 19p13.3 deletion in every individual patient. Table S3 presents the TCR β rearrangements of the clonal tumor cell population and the antibodies used for detecting/enrichment of the tumor cells. Table S4 shows chromosomal copy number alterations of *TP53* and *myc* in our SS samples. Table S5 gives a complete list of *E2A*-regulated genes in Se-Ax cells. Table S6 shows the overlap between our dataset and datasets derived from murine *E2A*-deficient cell types. Table S7 presents all detected sequence alterations within the *E2A* coding region. Table S8 gives an overview of the used CGH array platforms. Online supplemental material is available at <http://www.jem.org/cgi/content/full/jem.20101785/DC1>.

Funding was provided in part by Framework VII EU (European Union/BMBF-0315207A) grant, the Deutsche Forschungsgemeinschaft (TRR54), the Berliner Krebsgesellschaft, and the Max Planck Innovation Fonds. We thank Linda El-Ahmad, Franziska Hummel, Simone Kressmann, Katrin Tebel, and Arleta Frensel for excellent technical assistance, and Peter Rahn for cell sorting.

A. Steininger and M. Möbs designed and performed experiments and contributed to writing of the paper. I. Anagnostopoulos, M. Hummel, and H. Stein provided material and performed and interpreted immunohistochemistry analyses. K. Köchert, B. Lamprecht, and S. Kreher performed experiments and interpreted data. M. Beyer and C.D. Klemke provided material. E. Schrock designed and interpreted FISH analyses. J. Richter designed and interpreted bisulfite pyrosequencing analyses. B. Dörken, W. Sterry, E. Schrock, and M. Janz interpreted data and contributed to writing of the manuscript. R. Ullmann, S. Mathas, and C. Assaf designed the study, interpreted data, and wrote the manuscript.

The authors declare no competing financial interests.

Submitted: 27 August 2010

Accepted: 17 June 2011

REFERENCES

- Alimonti, A., A. Carracedo, J.G. Clohessy, L.C. Trotman, C. Nardella, A. Egia, L. Salmena, K. Sampieri, W.J. Haveman, E. Brogi, et al. 2010. Subtle variations in Pten dose determine cancer susceptibility. *Nat. Genet.* 42:454–458. doi:10.1038/ng.556
- Aspland, S.E., H.H. Bendall, and C. Murre. 2001. The role of E2A-PBX1 in leukemogenesis. *Oncogene*. 20:5708–5717. doi:10.1038/sj.onc.1204592
- Bain, G., I. Engel, E.C. Robanus Maandag, H.P. te Riele, J.R. Voland, L.L. Sharp, J. Chun, B. Huey, D. Pinkel, and C. Murre. 1997. E2A deficiency leads to abnormalities in alphabeta T-cell development and to rapid development of T-cell lymphomas. *Mol. Cell. Biol.* 17:4782–4791.
- Barrett, T., and R. Edgar. 2006. Gene expression omnibus: microarray data storage, submission, retrieval, and analysis. *Methods Enzymol.* 411:352–369. doi:10.1016/S0076-6879(06)11019-8
- Brochet, X., M.P. Lefranc, and V. Giudicelli. 2008. IMGT/V-QUEST: the highly customized and integrated system for IG and TR standardized V-J and V-D-J sequence analysis. *Nucleic Acids Res.* 36(Web Server issue):W503–W508. doi:10.1093/nar/gkn316
- Eckfeld, K., L. Hesson, M.D. Vos, I. Bieche, F. Latif, and G.J. Clark. 2004. RASSF4/AD037 is a potential ras effector/tumor suppressor of the RASSF family. *Cancer Res.* 64:8688–8693. doi:10.1158/0008-5472.CAN-04-2065
- Eischen, C.M., J.D. Weber, M.F. Roussel, C.J. Sherr, and J.L. Cleveland. 1999. Disruption of the ARF-Mdm2-p53 tumor suppressor pathway in Myc-induced lymphomagenesis. *Genes Dev.* 13:2658–2669. doi:10.1101/gad.13.20.2658
- Erdogan, F., W. Chen, M. Kirchoff, V.M. Kalscheuer, C. Hultschig, I. Müller, R. Schulz, C. Menzel, T. Bryndorf, H.H. Ropers, and R. Ullmann. 2006. Impact of low copy repeats on the generation of balanced and unbalanced chromosomal aberrations in mental retardation. *Cytogenet. Genome Res.* 115:247–253. doi:10.1159/000095921
- Herold, S., B. Herkert, and M. Eilers. 2009. Facilitating replication under stress: an oncogenic function of MYC? *Nat. Rev. Cancer.* 9:441–444. doi:10.1038/nrc2640
- Hu, M.G., A. Deshpande, M. Enos, D. Mao, E.A. Hinds, G.F. Hu, R. Chang, Z. Guo, M. Dose, C. Mao, et al. 2009. A requirement for cyclin-dependent kinase 6 in thymocyte development and tumorigenesis. *Cancer Res.* 69:810–818. doi:10.1158/0008-5472.CAN-08-2473
- Ikawa, T., H. Kawamoto, A.W. Goldrath, and C. Murre. 2006. E proteins and Notch signaling cooperate to promote T cell lineage specification and commitment. *J. Exp. Med.* 203:1329–1342. doi:10.1084/jem.20060268
- Kaltoft, K., S. Bisballe, H.F. Rasmussen, K. Thestrup-Pedersen, K. Thomsen, and W. Sterry. 1987. A continuous T-cell line from a patient with Sézary syndrome. *Arch. Dermatol. Res.* 279:293–298. doi:10.1007/BF00431220
- Kamstrup, M.R., L.M. Gjerdrum, E. Biskup, B.T. Lauenborg, E. Ralfkiaer, A. Woetmann, N. Ødum, and R. Gniadecki. 2010. Notch1 as a potential therapeutic target in cutaneous T-cell lymphoma. *Blood.* 116:2504–2512. doi:10.1182/blood-2009-12-260216
- Kari, L., A. Loboda, M. Nebozhyn, A.H. Rook, E.C. Vonderheid, C. Nichols, D. Virok, C. Chang, W.H. Hornig, J. Johnston, et al. 2003. Classification and prediction of survival in patients with the leukemic phase of cutaneous T cell lymphoma. *J. Exp. Med.* 197:1477–1488. doi:10.1084/jem.20021726
- Kee, B.L. 2009. E and ID proteins branch out. *Nat. Rev. Immunol.* 9:175–184. doi:10.1038/nri2507
- Koch, U., and F. Radtke. 2007. Notch and cancer: a double-edged sword. *Cell. Mol. Life Sci.* 64:2746–2762. doi:10.1007/s00018-007-7164-1
- Lamprecht, B., K. Walter, S. Kreher, R. Kumar, M. Hummel, D. Lenze, K. Köchert, M.A. Bouhlel, J. Richter, E. Soler, et al. 2010. Derepression of an endogenous long terminal repeat activates the CSF1R proto-oncogene in human lymphoma. *Nat. Med.* 16:571–579. doi:10.1038/nm.2129

- Lefranc, M.P., V. Giudicelli, C. Ginestoux, J. Jabado-Michaloud, G. Folch, F. Bellahcene, Y. Wu, E. Gemrot, X. Brochet, J. Lane, et al. 2009. IMGT, the international ImMunoGeneTics information system. *Nucleic Acids Res.* 37(Database issue):D1006–D1012. doi:10.1093/nar/gkn838
- Lietz, A., M. Janz, M. Sigvardsson, F. Jundt, B. Dörken, and S. Mathas. 2007. Loss of bHLH transcription factor E2A activity in primary effusion lymphoma confers resistance to apoptosis. *Br. J. Haematol.* 137:342–348. doi:10.1111/j.1365-2141.2007.06583.x
- Lockyer, P.J., S. Kupzig, and P.J. Cullen. 2001. CAPRI regulates Ca(2+)-dependent inactivation of the Ras-MAPK pathway. *Curr. Biol.* 11:981–986. doi:10.1016/S0960-9822(01)00261-5
- Mathas, S., M. Janz, F. Hummel, M. Hummel, B. Wollert-Wulf, S. Lusatis, I. Anagnostopoulos, A. Lietz, M. Sigvardsson, F. Jundt, et al. 2006. Intrinsic inhibition of transcription factor E2A by HLH proteins ABF-1 and Id2 mediates reprogramming of neoplastic B cells in Hodgkin lymphoma. *Nat. Immunol.* 7:207–215. doi:10.1038/ni1285
- Mathas, S., S. Kreher, K.J. Meaburn, K. Jöhrens, B. Lamprecht, C. Assaf, W. Sterry, M.E. Kadin, M. Daibata, S. Joos, et al. 2009. Gene deregulation and spatial genome reorganization near breakpoints prior to formation of translocations in anaplastic large cell lymphoma. *Proc. Natl. Acad. Sci. USA.* 106:5831–5836. doi:10.1073/pnas.0900912106
- Mellentin, J.D., C. Murre, T.A. Donlon, P.S. McCaw, S.D. Smith, A.J. Carroll, M.E. McDonald, D. Baltimore, and M.L. Cleary. 1989. The gene for enhancer binding proteins E12/E47 lies at the t(1;19) breakpoint in acute leukemias. *Science.* 246:379–382. doi:10.1126/science.2799390
- Min, J., A. Zaslavsky, G. Fedele, S.K. McLaughlin, E.E. Reczek, T. De Raedt, I. Guney, D.E. Strohlich, L.E. Macconail, R. Beroukhim, et al. 2010. An oncogene-tumor suppressor cascade drives metastatic prostate cancer by coordinately activating Ras and nuclear factor-kappaB. *Nat. Med.* 16:286–294. doi:10.1038/nm.2100
- Morrow, M.A., E.W. Mayer, C.A. Perez, M. Adlam, and G. Siu. 1999. Overexpression of the Helix-Loop-Helix protein Id2 blocks T cell development at multiple stages. *Mol. Immunol.* 36:491–503. doi:10.1016/S0161-5890(99)00071-1
- Murre, C. 2005. Helix-loop-helix proteins and lymphocyte development. *Nat. Immunol.* 6:1079–1086. doi:10.1038/ni1260
- Murre, C., P.S. McCaw, and D. Baltimore. 1989. A new DNA binding and dimerization motif in immunoglobulin enhancer binding, daughterless, MyoD, and myc proteins. *Cell.* 56:777–783. doi:10.1016/0092-8674(89)90682-X
- Nie, L., M. Xu, A. Vladimirova, and X.H. Sun. 2003. Notch-induced E2A ubiquitination and degradation are controlled by MAP kinase activities. *EMBO J.* 22:5780–5792. doi:10.1093/emboj/cdg567
- O'Neil, J., J. Shank, N. Cusson, C. Murre, and M. Kelliher. 2004. TAL1/SCL induces leukemia by inhibiting the transcriptional activity of E47/HEB. *Cancer Cell.* 5:587–596. doi:10.1016/j.ccr.2004.05.023
- Olshen, A.B., E.S. Venkatraman, R. Lucito, and M. Wigler. 2004. Circular binary segmentation for the analysis of array-based DNA copy number data. *Biostatistics.* 5:557–572. doi:10.1093/biostatistics/kxh008
- Park, S.T., G.P. Nolan, and X.H. Sun. 1999. Growth inhibition and apoptosis due to restoration of E2A activity in T cell acute lymphoblastic leukemia cells. *J. Exp. Med.* 189:501–508. doi:10.1084/jem.189.3.501
- Reschly, E.J., C. Spaulding, T. Vilimas, W.V. Graham, R.L. Brumbaugh, I. Aifantis, W.S. Pear, and B.L. Kee. 2006. Notch1 promotes survival of E2A-deficient T cell lymphomas through pre-T cell receptor-dependent and -independent mechanisms. *Blood.* 107:4115–4121. doi:10.1182/blood-2005-09-3551
- Schröck, E., and H. Padilla-Nash. 2000. Spectral karyotyping and multi-color fluorescence in situ hybridization reveal new tumor-specific chromosomal aberrations. *Semin. Hematol.* 37:334–347. doi:10.1016/S0037-1963(00)90014-3
- Schwartz, R., I. Engel, M. Fallahi-Sichani, H.T. Petrie, and C. Murre. 2006. Gene expression patterns define novel roles for E47 in cell cycle progression, cytokine-mediated signaling, and T lineage development. *Proc. Natl. Acad. Sci. USA.* 103:9976–9981. doi:10.1073/pnas.0603728103
- Sigvardsson, M., M. O'Riordan, and R. Grosschedl. 1997. EBF and E47 collaborate to induce expression of the endogenous immunoglobulin surrogate light chain genes. *Immunity.* 7:25–36. doi:10.1016/S1074-7613(00)80507-5
- van Dongen, J.J., A.W. Langerak, M. Brüggemann, P.A. Evans, M. Hummel, F.L. Lavender, E. Delabesse, F. Davi, E. Schuurink, R. Garcia-Sanz, et al. 2003. Design and standardization of PCR primers and protocols for detection of clonal immunoglobulin and T-cell receptor gene recombinations in suspect lymphoproliferations: report of the BIOMED-2 Concerted Action BMH4-CT98-3936. *Leukemia.* 17:2257–2317. doi:10.1038/sj.leu.2403202
- van Doorn, R., R. Dijkman, M.H. Vermeer, J.J. Out-Luiting, E.M. van der Raaij-Helmer, R. Willemze, and C.P. Tensen. 2004. Aberrant expression of the tyrosine kinase receptor EphA4 and the transcription factor twist in Sézary syndrome identified by gene expression analysis. *Cancer Res.* 64:5578–5586. doi:10.1158/0008-5472.CAN-04-1253
- Vermeer, M.H., R. van Doorn, R. Dijkman, X. Mao, S. Whittaker, P.C. van Voorst Vader, M.J. Gerritsen, M.L. Geerts, S. Gelrich, O. Söderberg, et al. 2008. Novel and highly recurrent chromosomal alterations in Sézary syndrome. *Cancer Res.* 68:2689–2698. doi:10.1158/0008-5472.CAN-07-6398
- Willemze, R., E.S. Jaffe, G. Burg, L. Cerroni, E. Berti, S.H. Swerdlow, E. Ralfkiaer, S. Chimenti, J.L. Diaz-Perez, L.M. Duncan, et al. 2005. WHO-EORTC classification for cutaneous lymphomas. *Blood.* 105:3768–3785. doi:10.1182/blood-2004-09-3502
- Yan, W., A.Z. Young, V.C. Soares, R. Kelley, R. Benezra, and Y. Zhuang. 1997. High incidence of T-cell tumors in E2A-null mice and E2A/Id1 double-knockout mice. *Mol. Cell. Biol.* 17:7317–7327.

SUPPLEMENTAL MATERIAL

Steininger et al., <http://www.jem.org/cgi/content/full/jem.20101785/DC1>

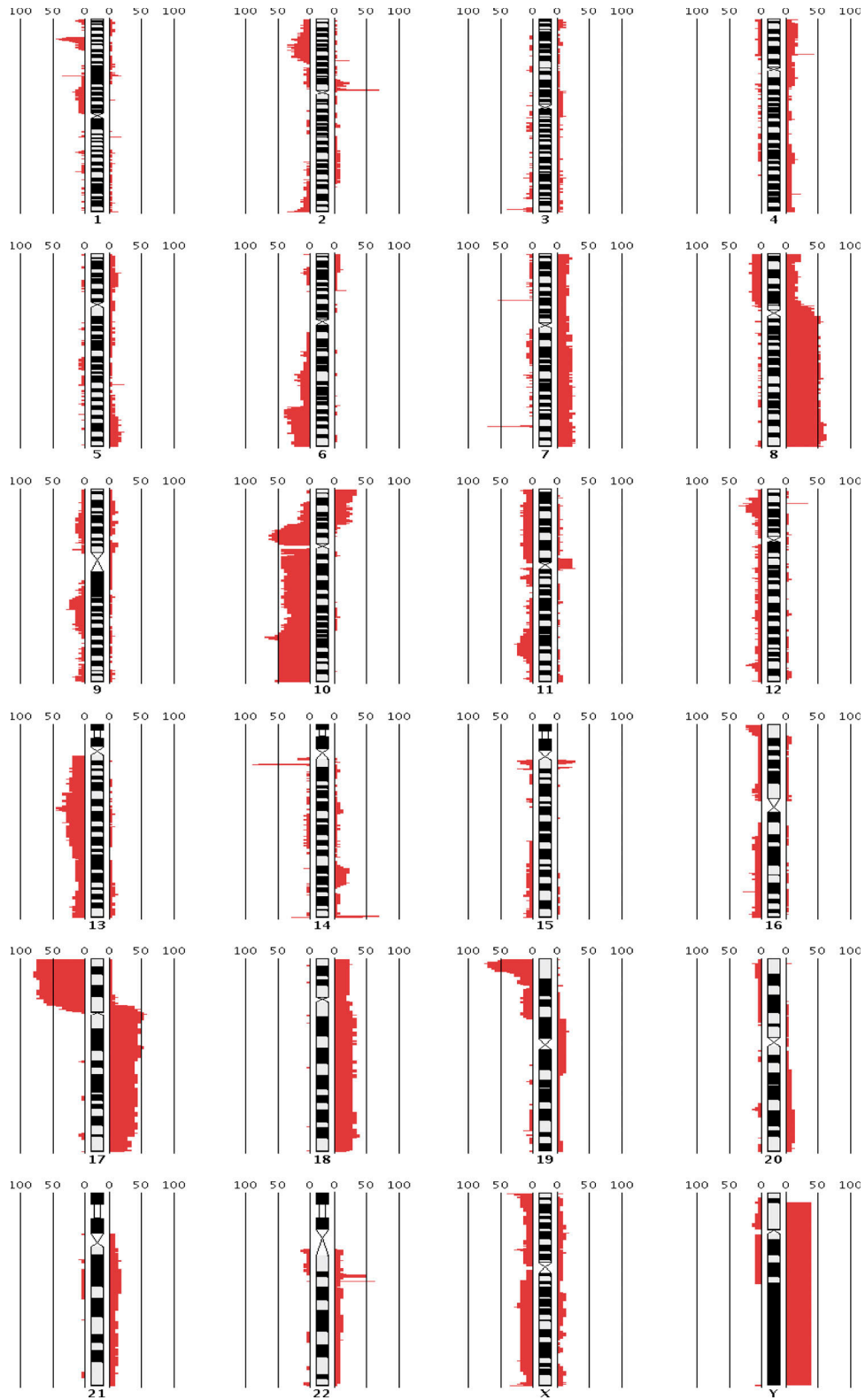


Figure S1. DNA copy number changes detected in tumor cells of 20 patients with SS. The frequency of chromosomal gains and losses in percentage of studied cases is shown to the right and to the left, respectively.

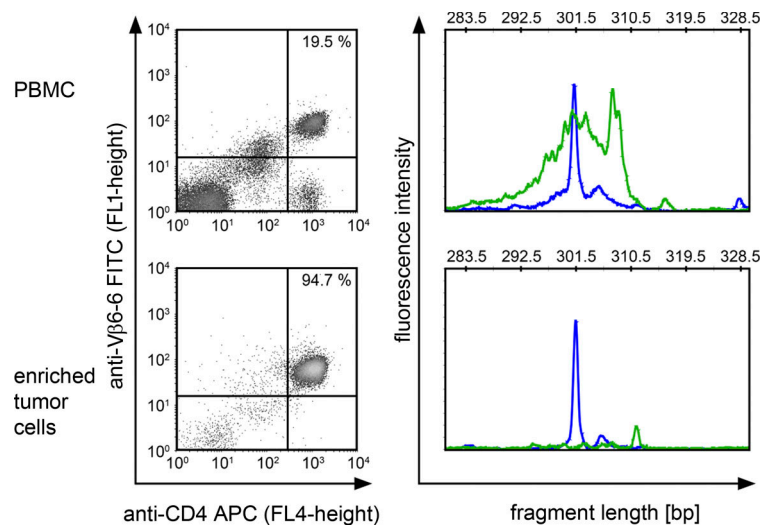


Figure S2. Tumor cell enrichment by magnetic cell sorting. PBMCs of patient 16 were analyzed before (top) and after (bottom) enrichment of tumor cells by magnetic sorting of $V\beta 6-6^+$ cells for CGH analysis. (left) Flow cytometric analysis of cells after staining with APC-labeled anti-CD4 and FITC-labeled anti- $V\beta 6-6$ antibodies. The percentage of $CD4^+V\beta 6-6^+$ cells is indicated. (right) Clonality analysis of T cells. Shown are the fluorescent fragment analysis profiles of "reaction 3" of the TCR β -rearrangement PCR showing a dominant clonal peak (for details on clonality analysis refer to Materials and methods). The dominant (blue) peak is identical in the unsorted and the enriched $V\beta 6-6^+$ cell sample, demonstrating that these cells represent the clonally expanded tumor cell population. Green peaks indicate amplification of rearrangements involving J β 1 gene segments; blue peaks indicate amplification of rearrangements involving J β 2 segments.

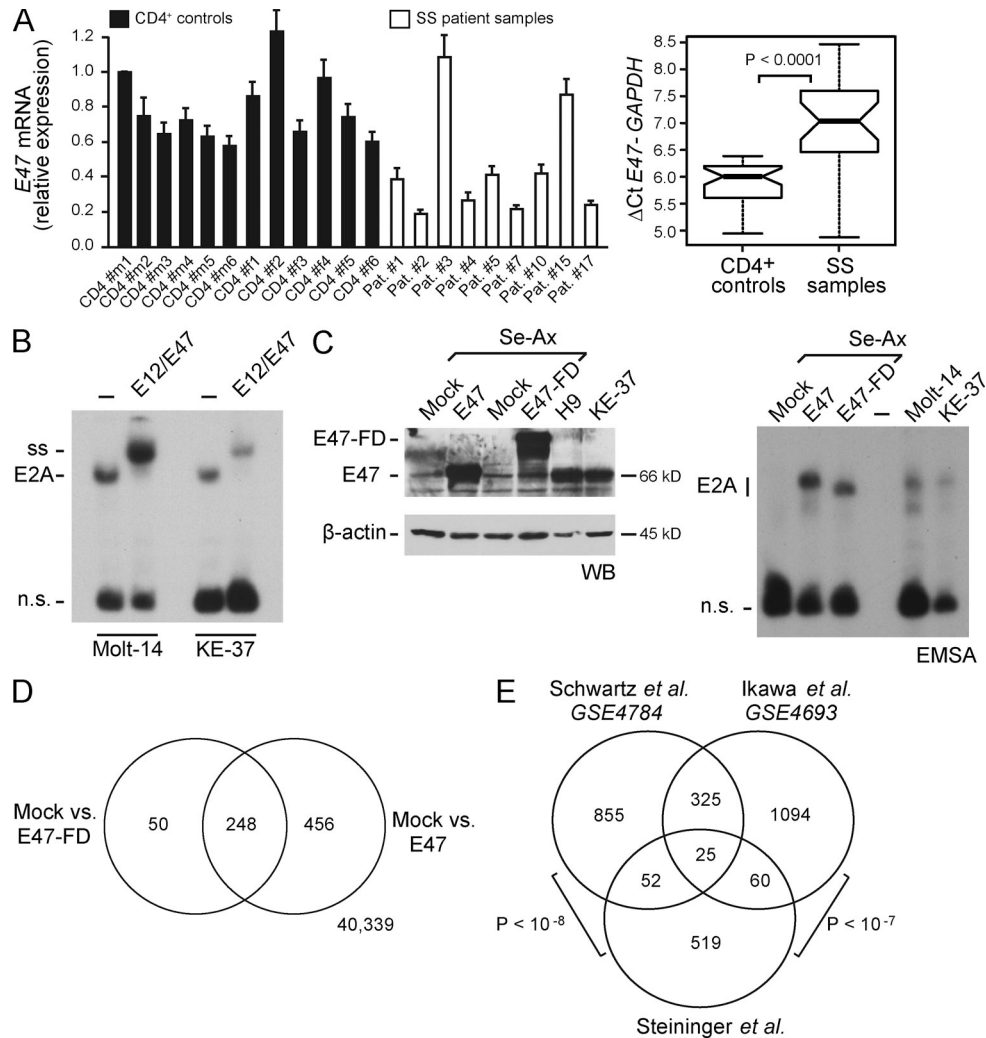


Figure S3. Expression of E47 mRNA in SS patient samples; E2A EMSA and protein expression analysis after E2A reconstitution of Se Ax cells; and gene expression analysis after E2A reconstitution. (A) Quantification of E2A mRNA levels by real-time PCR in CD4⁺ T lymphocytes from healthy volunteers and purified leukemic SS cells from various patients, as indicated. Left, E2A mRNA expression in various samples was analyzed relative to GAPDH by quantitative real-time RT-PCR using primers recognizing the E2A splice variant E47. Right, box plot presentation of the comparison of ΔCt values of E2A in CD4⁺ controls and SS patient samples. Results are shown for one of two independent experiments performed. (B) Specificity control of DNA bound complexes by supershift analysis. EMSA of nuclear extracts of Molt-14 and KE-37 cells without preincubation (-) or with preincubation with antibody to E2A (E12/E47). Data show EMSA of E2A-containing complexes with the μE5 element as probe. Positions of E2A complexes and complexes supershifted (ss) with antibody to E2A are indicated. n.s., nonspecific complexes. (C) Se-Ax cells were transfected with Mock plasmid (control) or plasmids encoding myc-tagged E47 (E47) or E47-FD, as indicated, along with pEGFP. 48 h after transfection, EGFP⁺ cells were enriched and protein extracts were prepared. Left, E47 and E47-FD protein expression in purified transfected cells was analyzed by immunoblotting, H9 and KE-37 cells were analyzed as controls. Right, E2A DNA binding activity in purified Se-Ax cells and Molt-14 and KE-37 control cell lines was analyzed by EMSA as described in Fig. 1 F. Results are shown for one of four independent experiments performed. (D) Se-Ax cells were transfected and purified as described in C. mRNA was extracted and gene expression profiling was performed using Agilent Whole Genome 4 × 44K arrays. Background corrected and normalized intensity values were then used for gene-wise linear model fitting using LIMMA, P values were adjusted for multiple testing using the method from Benjamini and Hochberg. The number of significantly deregulated genes (adjusted P value ≤ 0.05) with a \log_2 -fold change of ≤ 1 or ≥ -1 and the according overlap of the comparisons Mock vs. E47-FD and Mock vs. E47 are shown as Venn diagram. Results were obtained from two independent experiments. (E) To compare the entire spectrum of E2A-regulated genes in our microarray analyses of Se-Ax cells after E47 reconstitution with those regulated in murine lymphoid cells, we compared our data with the datasets of Schwartz et al. (2006; GEO accession no. GSE4784) and Ikawa et al. (2006; GEO accession no. GSE4693). These microarray datasets were generated with murine E2A-deficient T cell lymphoma cells and murine E2A-deficient hematopoietic progenitor cells, respectively. For all datasets, genes were deemed significantly regulated, when they showed a fold change in expression of at least > 1.5 or < 0.5 . The mouse-identifiers for the features of both GSE4784 and GSE4693 were mapped to human homologues for subsequent analysis of the overlap of regulated genes. The Venn diagram depicted shows the overlap of all genes that were up-regulated at least 1.5-fold in either dataset (of the 7 genes in our dataset, that were down-regulated at least 0.5-fold, none was found to be down-regulated to at least this degree in any of the other two datasets). This diagram shows that the overlap of our dataset with either of the other datasets is significant as calculated by hypergeometric test.

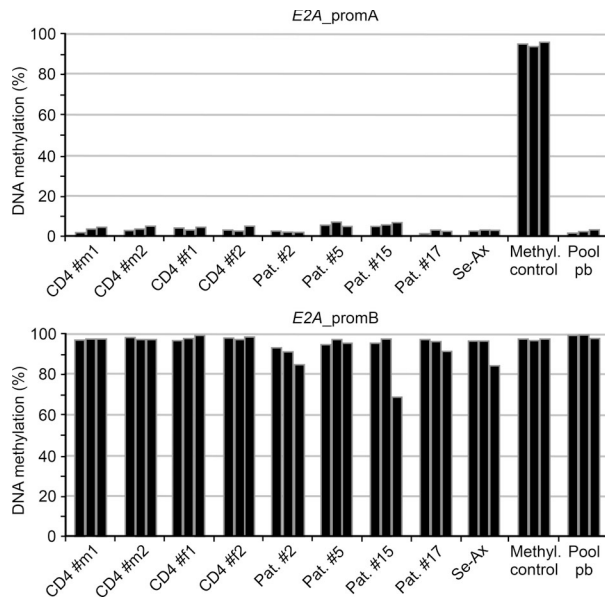


Figure S4. Methylation of two regions within the promoter region of *E2A* in SS patient samples compared with purified CD4⁺ T lymphocytes from healthy volunteers. Three CpGs of the *E2A* promoter region A (*E2A_promA*) and region B (*E2A_promB*) were analyzed by bisulfite pyrosequencing, respectively. For each sample, the DNA methylation is shown in percentage for each individual CpG site. Methyl. Control, in vitro methylated DNA; pool pb, pooled DNA isolated from PBMCs.

Table S1. Detailed patient information

Patient no.	Sex	Identical TCR-R in blood and skin*	Time point of blood sample (MM/YY)	Age in years	Peripheral blood parameters					Treatment before time point of blood sample
					WBC count/nl	% atypical cells (Sézary cells)	% CD4 ⁺ /CD3 ⁺	CD4 ⁺ /CD8 ⁺ ratio	% Vβ ⁺ /CD4 ⁺	
1	F	+	03/99	76	6.4	0	92	21	89	UVB, Pr
2	F	+	12/02	67	20.9	80	99	99	n.d.	Ch+P, IFN
3	F	n.d.	08/99	95	20.9	64	>99	49	>99	-
4	M	+	01/05 ^a	73	22.2	60	>99	665	99	UV, ECP
			02/05	73	22.7	76	96	712	n.d.	UV, ECP
5	F	n.d.	02/00	58	28.7	59	>99	94	98	-
6	M	+	10/09	59	31.1	33	99	136	n.d.	IFN, ECP
7	M	+	01/07 ^a	59	12.6	31	>99	63	97	IFN+ECP, Bex+SAHA, Ch+Pr
			03/07	59	23.0	33	99	321	n.d.	IFN+ECP, Bex+SAHA, Ch+Pr, αCD52
8	M	+	10/09	89	7.5	0	91	n.d.	74	PUVA
9	M	+	08/02	67	17.2	26	91	98	81	CyA, PUVA, IFN, ECP
10	M	+	02/03	74	13.2	25	97	29	93	PUVA, IFN
11	F	n.d.	08/00	86	6.9	21	97	24	96	PUVA Cyc+Pr, Cyc+Pr+V, Ch+Pr
			11/00 ^a	86	4.5	n.d.	94	n.d.	n.d.	PUVA Cyc+Pr, Cyc+Pr+V, Ch+Pr
12	M	n.d.	04/02	52	8.0	16	>99	n.d.	n.d.	PUVA, ECP, IFN, Dx, MTX
13	F	+	08/02	79	17.2	28	94	49	68	PUVA, Ch+Pr
14	F	n.d.	08/99	65	21.3	72	99	90	n.d.	ECP
15	F	+	08/07 ^a	64	21.3	n.d.	95	n.d.	n.d.	IFN, ECP, Ch+P, PUVA, MTX, Cyc, Bex+SAHA
			03/08	64	30.1	28	n.d.	n.d.	n.d.	IFN, ECP, Ch+P, PUVA, MTX, Cyc, Bex+SAHA
16	F	+	08/08	79	9.2	8	92	20	84	ECP, IFN
			01/09 ^a	79	7.6	n.d.	91	15	n.d.	ECP, IFN
17	F	+	09/08	72	8.1	25	99	197	94	ECP, PUVA, IFN
18	M	+	03/97	62	43.0	44	n.d.	n.d.	n.d.	PUVA
19	M	+	01/10	49	11.9	n.d.	97	48	96	-
20	F	+	03/10	62	11.8	n.d.	96	31.9	89	ECP

TCR-R, T cell receptor rearrangement; WBC, white blood cell; Ac, acitretin; Bex, bexarotene; Ch, chlorambucil; CyA, cyclosporin A; Cyc, cyclophosphamide; Dx, doxorubicin; ECP, extracorporeal photopheresis; Flu, fludarabine; MTX, methotrexate; Pr, prednisone; PUVA, psoralen + irradiation with long wave ultraviolet light; SAHA, suberoylanilide hydroxamic acid; UV, irradiation with ultraviolet light (wave length not specified); UVB, irradiation with short wave ultraviolet light; V, vincristine; αCD52, Alemtuzumab (humanized monoclonal antibody targeting the CD52 antigen); n.d., not determined; *, as determined by TCR-rearrangement PCR and subsequent fluorescent fragment analysis.

^aSamples used for FISH analyses

Table S2. Chromosomal positions of 19p deletions including *E2A*

Patient no.	19p deletion	
	start (bp)	end (bp)
1	19pter	5634354
2	19pter	8313679
3	1368087	4038576
4	19pter	4312210
5	329606	19692685
6	19pter	1881426
7	19pter	3413889
8	902763	4116979
9	-	-
10	-	-
11	265457	4110578
12	-	-
13	794978	4424528
14	-	-
15	-	-
16	-	-
17	19pter	5763726
18	19pter	2824434
19	19pter	4033360
20	19pter	7992388

Chromosomal positions (HG18) are based on circular binary segmentation and a \log_2 threshold of -0.2 .

Table S3. Sequence analysis of the clonal TCR β -rearrangements obtained from patients with SS

Patient no.	3'V β -region	N1	D β	N2	5'J β -region	V β	D β	J β	Pr	Ab clone
1	TGTGCCAGTAGT.....	CTCC	.GGACAGGG...	AG	CTCCTATAATTCACCCCTCCACTTT	19	1	1-6	+	E17.5F3.15.13
2	TGTGCCAGCTCACCAC.	TAGCGGAGGG	CCCGGGAGCTGTTTTTT	18	2	2-2	+	BA62.6*
3	TGTGCCAGCAGT.....	C	.GGACTAGC.....	CTACTATATTTTT	2	2	2-3	-	n.a.
	TGTGCCAGTAG.....	CACC	GGGACTA.....	CTATCACCGGGAGCTGTTTTTT	19	2	2-2	+	E17.5F3.15.13
4	TGTGCCAGCAGT.....	CCAACCTT		TTCACCCCTCCACTTT	6-5	-	1-6	+	IMMU 222
5	TGTGCCAGTAGT.....	GGAGGG...	CTGGGGGAAAACTGTTTTTT	19	1	1-4	+	E17.5F3.15.13
6	TGTGCCAGTAGATA..	AGA	GGGA.....	GTCT	CTCTGGAACACCATATATTTT	19	1	1-3	+	E17.5F3.15.13
7	TGTGCCAGCAGCC....	CTCGTCTAGCGGAG..	AGATCATTCACTACTTC	3-1	2	2-4	+	FIN9
8	TGTGCCAGC.....	GTCG	GGGAC.....	CCATAACTCTGGCCCCAGCATTTT	2	1	1-5	-	n.a.
		CCTCC								
	TGCAGTGCTAG.	AGAGGGGGC	TCCAGATACGCAGTATTTT	20	1	2-3	+	MPB2D5
9	TGTGCCAGCAGCC....	CCCA	.GGACAGGG...	CGTATGGCTACACCTTC	3-1	1	1-2	+	FIN9
10	TGTGCCAGCAGTGA...	GGTTA	..GACTAGCGG.....	T	...CTACAATGAGCAGTTCTTC	2	2	2-1	+	IMMU 546
11	TGCGCCAGC.....	CGC	..GACAG.....		CTCCTACGAGCAGTACTTC	5-1	1	2-7	+	IMMU 157
12	TGTGCCAGCAGCTTGG		.GGACAGG....	CCT	CTCTGGAACACCATATATTTT	5-4	1	1-3	+	~
13	TGTGCCAGCAGCTTGG	CAAG		CACTGAAGCTTTCTTT	5-6	-	1-1	+	36213
14	TGTGCCAGCAGCTTAG.	GTCCAGGAGGCCGGG...	AGACTGTTTTTT	7-9	2	2-2	-	n.a.
15	TGTGCCAGCAGCTTGG	CCACCCCTAG.....	CAATGAGCAGTTCTTC	5-4	2	2-1	+	~
16	TGTGCCAGCAGTTAC..	CCCAG.....		CTCCTACAATGAGCAGTTCTTC	6-6	1	2-1	+	JU74.3
17	TGTGCCAGCAGTTTAG.	GGCAGGG...	CACTGAAGCTTTCTTT	12-3	1	1-1	+	56C5.2
18	Sequence analysis not done.									
19	TGCAGTGCTAG....	TTT	GGGACTAGCGGG...	AATGAGCAGTTCTTC	20	2	2-1	+	MPB2D5
20	TGTGCCAGCAGTTTATC	GGGC	..GACAG.....	ACATAATTCACCCCTCCACTTT	27	1	1-6	+	CAS1.1.3
		GCGGCT								

The representative clone-specific sequence of the junctional region is shown. The nomenclature of the corresponding V, D, and J germline segments is based on the international ImMunoGeneTics information system. Pr, Productive gene rearrangement; ~, no specific antibody available. *, no specific binding of the antibody within the CD3/CD4 double-positive cell fraction; n.a., not applicable (unproductive TCR β -rearrangement).

Table S4. Chromosomal gains and losses of *TP53* and *MYC*

Patient no.	Array CGH analysis		FISH analysis
			(number of cells with deletion/number of analyzed cells)
	Loss of	Gain of	Loss of
	<i>TP53</i>	<i>MYC</i>	<i>TP53</i>
1	yes	no	yes (195/200)
2	yes	yes	n. n.d
3	yes	no	yes (199/200)
4 ^b	yes	yes	yes (200/200)
5 ^a	yes	yes	yes (195/200)
6 ^a	yes	no	n.d.
7 ^b	yes	yes	no (0/200)
8 ^a	yes	yes	n.d.
9	yes	yes	yes (100/200)
10	yes	no	yes (200/200)
11 ^{a,b}	yes	yes	yes (196/200)
12	no	yes	n.d.
13	no	yes	no (1/200)
14	yes	no	n.d.
15 ^b	no	yes	yes (loss 37/200, gain 48/200)
16 ^{a,b}	yes	no	yes (178/200)
17 ^a	yes	yes	yes (193/200)
18	yes	yes	n.d.
19 ^a	yes	yes	n.d.
20 ^a	no	no	n.d.
Se-Ax	yes	yes	yes (100/100)

n.d., not determined.

^aCGH was performed on enriched tumor cells^bCGH and FISH analyses were performed with samples from different time points (see Table S1).

Table S5. E2A-regulated genes in Se-Ax cells

Agilent probe ID	Log ₂ -fold change: E47-FD vs. Mock	Log ₂ -fold change: E47 vs. Mock	Adjusted p-value: E47-FD vs. Mock	Adjusted p-value: E47 vs. Mock	Gene symbol
A_23_P74012	9.36	10.15	1.00E-06	0.00	SPRR1A
A_23_P93348	7.15	7.19	0.00	0.00	LTB
A_23_P104555	5.62	6.82	3.00E-06	0.00	ANKRD2
A_23_P200579	5.61	4.63	0.00	0.00	ELA3B
A_23_P428129	4.95	6.28	3.00E-06	0.00	CDKN1C
A_23_P34700	4.67	4.08	6.20E-05	4.50E-05	TNNT2
A_23_P112481	4.54	4.71	0.00	0.00	AQP3
A_32_P94444	4.5	2.01	0.00	0.04	PRSS2
A_23_P111766	4.4	1.95	0.00	0.04	A_23_P111766
A_24_P927304	4.38	3.79	5.60E-05	4.10E-05	TNNT2
A_23_P148737	4.28	5.18	0.01	0.00	MYBPH
A_23_P218047	4.18	4.92	3.30E-05	4.00E-06	KRT5
A_23_P27133	4.15	6.66	0.01	0.00	KRT15
A_23_P95213	4.05	5.1	0.00	9.00E-06	SFTPC
A_23_P132175	4.05	6.57	1.90E-05	0.00	RTN4R
A_23_P112482	3.95	4.06	0.00	0.00	AQP3
A_23_P106024	3.91	6.47	0.00	0.00	JAG2
A_23_P48088	3.9	4.06	1.90E-05	5.00E-06	CD27
A_23_P64051	3.9	6.19	2.00E-05	0.00	CDC42BPG
A_23_P1912	3.86	2.27	0.00	0.01	ZP1
A_32_P16315	3.68	2.85	0.00	0.00	ENST00000272035
A_23_P96158	3.55	5.01	0.02	0.00	KRT17
A_32_P103669	3.54	5.14	0.00	0.00	GOLGA8E
A_24_P257022	3.53	3.02	0.00	0.00	TNNT2
A_23_P115261	3.53	2.45	0.00	0.01	AGT
A_24_P610945	3.39	4.97	0.02	0.00	ENST00000311208
A_23_P17134	3.32	3.18	8.30E-05	3.50E-05	MAL
A_32_P59302	3.3	3.6	0.00	8.70E-05	HIVEP3
A_23_P140884	3.27	2.74	0.01	0.01	BC014971
A_23_P102113	3.2	2.58	3.00E-06	3.00E-06	WNT10A
A_32_P73507	3.15	2.85	1.00E-06	0.00	THC2647902
A_23_P332960	3.12	4.37	3.30E-05	1.00E-06	TMEM80
A_24_P177236	3.1	5.03	0.00	7.40E-05	CABP7
A_23_P250102	3.09	1.76	1.50E-05	0.00	CAND2
A_24_P887857	3.09	4.55	0.04	0.00	LOC650517
A_24_P62469	3.08	5.27	9.30E-05	1.00E-06	PLCH2
A_23_P39955	3.04	2.26	0.00	0.00	ACTG2
A_23_P363769	3.01	3.65	0.01	0.00	KRT86
A_24_P265346	2.95	4.56	0.04	0.00	KRT14
A_23_P500010	2.92	3.71	0.02	0.00	KLK12
A_23_P5845	2.91	3.52	3.00E-06	0.00	KHK
A_23_P372834	2.88	2.5	0.00	0.00	AQP1
A_23_P102117	2.88	2.27	1.30E-05	1.50E-05	WNT10A
A_23_P210482	2.88	2.76	1.00E-06	0.00	ADA
A_23_P421306	2.86	3.2	2.00E-06	0.00	SYT12
A_23_P163492	2.85	5.56	0.00	8.00E-06	BAIAP3
A_23_P304897	2.8	5.39	0.00	2.20E-05	BDKRB2
A_23_P210176	2.78	1.58	0.00	0.01	ITGA6

Se-Ax cells were transfected as described in Fig. S3. Table of all genes that showed at least a log₂-fold change > 1.0 or < -1.0 and an adjusted p-value of P < 0.05 in the comparison E47-FD vs. Mock. According log₂-fold changes and adjusted p-values of the comparison E47 vs. Mock are also stated. Calculation of adjusted p-values was done as described in Fig. S3.

Table S5. E2A-regulated genes in Se-Ax cells (Continued)

Agilent probe ID	Log ₂ -fold change: E47-FD vs. Mock	Log ₂ -fold change: E47 vs. Mock	Adjusted p-value: E47-FD vs. Mock	Adjusted p-value: E47 vs. Mock	Gene symbol
A_24_P8371	2.76	3.76	0.00	0.00	LOC124976
A_23_P69293	2.76	2.55	1.00E-06	1.00E-06	CHDH
A_23_P207345	2.76	3.52	6.00E-05	5.00E-06	ADAM11
A_23_P39925	2.71	3.86	0.00	5.00E-06	DYSF
A_24_P589028	2.7	4.08	0.01	0.00	AK026750
A_23_P348208	2.61	3.5	0.00	0.00	SPRR1A
A_23_P111860	2.6	4.75	0.00	6.00E-06	FLJ10324
A_23_P37702	2.54	5.24	0.00	6.00E-06	TPSAB1
A_23_P107401	2.51	1.41	0.00	0.00	TIMP2
A_23_P16252	2.5	3.28	0.00	7.70E-05	KLK1
A_23_P129695	2.49	2.96	0.04	0.01	VASN
A_23_P142878	2.49	2.31	0.00	0.00	ATOH8
A_23_P21495	2.46	5.15	3.30E-05	0.00	FCGBP
A_32_P38093	2.39	2.82	0.00	6.90E-05	THC2632909
A_23_P39931	2.36	3.39	3.50E-05	1.00E-06	DYSF
A_23_P64661	2.36	2.56	0.00	4.40E-05	ARHGAP9
A_24_P382579	2.35	2.89	0.01	0.00	OXT
A_23_P146554	2.35	2.91	0.00	0.00	PTGDS
A_23_P159237	2.35	3.93	0.02	0.00	GPR20
A_23_P41390	2.34	3.56	8.30E-05	2.00E-06	SH3TC1
A_23_P44335	2.31	2.69	1.20E-05	1.00E-06	ENTPD8
A_23_P22143	2.25	5.79	0.00	5.00E-06	PDE6B
A_23_P319583	2.25	3.00	0.00	4.40E-05	RIMS3
A_23_P163682	2.24	3.67	0.01	0.00	RHBDF1
A_23_P101392	2.22	3.09	0.00	3.10E-05	TMEM38A
A_24_P329795	2.22	2.28	0.04	0.01	C10orf10
A_23_P413641	2.2	2.78	9.70E-05	7.00E-06	PREX1
A_23_P112798	2.19	5.21	3.00E-06	0.00	CRIP2
A_23_P24104	2.19	2.05	0.01	0.00	PLAU
A_23_P33196	2.19	1.68	0.00	0.00	COL5A2
A_23_P112774	2.16	4.58	0.00	3.00E-06	PTP4A3
A_23_P161769	2.16	4.22	0.00	3.00E-06	FXD2
A_23_P53257	2.14	3.18	0.01	0.00	AVIL
A_24_P295590	2.13	2.22	3.00E-06	1.00E-06	RASSF4
A_24_P357847	2.12	1.49	8.00E-06	1.80E-05	BC030813
A_23_P33511	2.09	4.29	0.01	3.50E-05	AX721087
A_32_P48825	2.08	2.27	0.01	0.00	KRT72
A_32_P39440	2.07	1.53	2.00E-06	3.00E-06	BC030813
A_24_P31165	2.07	1.78	0.00	0.00	GFAP
A_32_P159192	2.06	1.48	3.00E-06	6.00E-06	ENST00000295339
A_24_P142118	2.03	1.31	7.00E-06	3.00E-05	THBS1
A_24_P378019	2.02	3.48	0.03	0.00	IRF7
A_24_P364838	2.01	3.34	5.90E-05	1.00E-06	SLC9A3R2
A_32_P148118	2.00	1.51	1.90E-05	3.30E-05	ENST00000331696
A_23_P98786	1.99	3.93	0.03	0.00	MYO7A
A_32_P86763	1.99	3.54	0.00	1.70E-05	TGM2
A_23_P75260	1.98	2.08	5.90E-05	1.40E-05	RASSF4
A_23_P21382	1.95	5.56	0.00	0.00	LAMB2
A_32_P98072	1.95	2.17	0.04	0.01	ENST00000368804

Se-Ax cells were transfected as described in Fig. S3. Table of all genes that showed at least a log₂-fold change > 1.0 or < -1.0 and an adjusted p-value of P < 0.05 in the comparison E47-FD vs. Mock. According log₂-fold changes and adjusted p-values of the comparison E47 vs. Mock are also stated. Calculation of adjusted p-values was done as described in Fig. S3.

Table S5. E2A-regulated genes in Se-Ax cells (Continued)

Agilent probe ID	Log ₂ -fold change: E47-FD vs. Mock	Log ₂ -fold change: E47 vs. Mock	Adjusted p-value: E47-FD vs. Mock	Adjusted p-value: E47 vs. Mock	Gene symbol
A_24_P122921	1.93	2.28	8.00E-06	1.00E-06	BCL2L11
A_23_P206212	1.93	1.17	1.90E-05	0.00	THBS1
A_23_P357185	1.92	1.68	6.00E-06	4.00E-06	CHDH
A_24_P923251	1.91	3.18	0.01	0.00	TGM2
A_23_P147326	1.9	1.88	0.02	0.01	SERINC2
A_23_P360874	1.89	2.67	0.00	4.90E-05	DKFZp434K1815
A_24_P140608	1.88	1.58	0.00	0.00	HBEGF
A_23_P34804	1.88	1.53	3.50E-05	3.90E-05	NTRK1
A_23_P105562	1.86	3.54	0.00	2.10E-05	VWF
A_23_P258887	1.86	2.84	0.00	0.00	ALDH1L1
A_24_P303524	1.84	3.42	0.03	0.00	MICALL2
A_23_P138495	1.82	2.81	1.20E-05	0.00	PTPRE
A_24_P383609	1.82	2.61	0.00	0.00	NANOS1
A_23_P346093	1.81	2.52	0.00	4.10E-05	TMC8
A_23_P150547	1.8	0.81	0.00	0.02	PGA3
A_23_P217845	1.8	1.84	0.01	0.00	RGS16
A_23_P160800	1.8	1.25	0.02	0.04	NROB2
A_24_P639701	1.8	1.25	1.30E-05	3.50E-05	AY062331
A_24_P943263	1.79	3.1	0.00	4.50E-05	RASA4
A_23_P61688	1.78	2.87	3.50E-05	1.00E-06	SLC12A7
A_24_P213494	1.78	3.08	0.00	3.60E-05	PTPRE
A_23_P320578	1.77	1.77	0.00	0.00	RGS16
A_23_P21800	1.75	1.21	6.50E-05	0.00	BC032451
A_24_P272146	1.75	1.31	3.00E-06	6.00E-06	IGKC
A_24_P32295	1.73	3.06	0.00	8.00E-06	C19orf36
A_24_P490109	1.73	1.34	2.70E-05	3.80E-05	A_24_P490109
A_23_P316612	1.73	4.44	0.00	6.00E-06	GLIS1
A_24_P265506	1.72	1.2	1.20E-05	2.90E-05	NTRK1
A_23_P429977	1.72	4.02	5.00E-06	0.00	KCNQ1
A_23_P17316	1.71	5.29	0.00	1.00E-06	C20orf58
A_23_P416581	1.71	4.69	0.00	0.00	GNAZ
A_23_P128230	1.69	2.99	0.02	0.00	NR4A1
A_23_P84596	1.69	1.53	0.00	0.00	MGC29506
A_23_P147822	1.69	2.46	0.01	0.00	EPS8L2
A_32_P46238	1.66	2.58	0.00	3.10E-05	LOC339240
A_24_P402510	1.66	2.91	0.02	0.00	SAMD11
A_24_P66578	1.65	1.21	0.00	0.00	ENST00000377221
A_24_P90349	1.65	2.55	0.01	0.00	TMEM80
A_23_P349966	1.65	2.16	0.01	0.00	TMEM130
A_24_P182461	1.64	1.55	0.02	0.01	IGSF3
A_23_P252306	1.63	1.06	0.00	0.00	ID1
A_23_P4962	1.61	2.82	0.00	1.70E-05	NLRP5
A_24_P924631	1.61	1.33	0.00	0.00	THC2500892
A_23_P413051	1.6	0.99	0.01	0.02	NOX01
A_23_P360240	1.6	2.14	0.00	7.70E-05	MYEOV
A_23_P165778	1.59	1.18	0.02	0.03	MLPH
A_24_P823096	1.58	2.34	0.01	0.00	AL109708
A_24_P571824	1.58	2.85	0.01	0.00	A_24_P571824
A_23_P341860	1.56	3.53	0.00	1.00E-06	BC073815

Se-Ax cells were transfected as described in Fig. S3. Table of all genes that showed at least a log₂-fold change > 1.0 or < -1.0 and an adjusted p-value of P < 0.05 in the comparison E47-FD vs. Mock. According log₂-fold changes and adjusted p-values of the comparison E47 vs. Mock are also stated. Calculation of adjusted p-values was done as described in Fig. S3.

Table S5. E2A-regulated genes in Se-Ax cells (Continued)

Agilent probe ID	Log ₂ -fold change: E47-FD vs. Mock	Log ₂ -fold change: E47 vs. Mock	Adjusted p-value: E47-FD vs. Mock	Adjusted p-value: E47 vs. Mock	Gene symbol
A_24_P226008	1.56	1.94	0.00	0.00	MGLL
A_23_P126278	1.55	1.16	0.00	0.00	CHIT1
A_32_P42236	1.54	3.35	0.00	5.00E-06	BM461836
A_23_P61810	1.53	3.99	0.02	3.50E-05	BAIAP2
A_23_P371039	1.52	3.93	0.01	1.50E-05	NTSR1
A_23_P29282	1.51	2.24	0.00	7.00E-06	NPTXR
A_24_P196562	1.5	3.27	0.00	1.00E-06	FXYD2
A_23_P38630	1.5	0.96	0.01	0.03	SSTR2
A_23_P72330	1.5	1.13	0.00	0.00	A_23_P72330
A_24_P880000	1.49	1.22	1.50E-05	1.50E-05	AF088004
A_23_P319598	1.48	2.62	0.02	0.00	C4BPB
A_23_P159227	1.48	1.76	0.01	0.00	ADAM15
A_23_P143981	1.47	3.63	0.01	9.00E-06	FBLN2
A_23_P500741	1.47	4.65	0.00	1.00E-06	CBFA2T3
A_24_P35400	1.46	3.88	6.50E-05	0.00	SARDH
A_23_P35456	1.46	1.87	0.00	0.00	SH3PXD2A
A_23_P11787	1.46	4.16	0.00	0.00	WNT4
A_24_P331704	1.45	2.49	0.00	4.10E-05	KRT80
A_24_P395966	1.45	1.55	3.00E-05	6.00E-06	ZBP1
A_23_P50674	1.45	2.61	0.02	0.00	C19orf36
A_23_P35330	1.44	1.46	0.00	0.00	HIVEP3
A_23_P10559	1.44	2.65	0.00	1.00E-06	AATK
A_23_P66073	1.44	2.45	0.02	0.00	AF113013
A_23_P256158	1.43	2.95	0.00	2.00E-06	ADRA2C
A_23_P32500	1.43	4.1	0.00	3.00E-06	STAB1
A_23_P422851	1.42	1.37	0.00	0.00	CABLES1
A_23_P14769	1.42	0.66	0.00	0.01	FES
A_23_P170534	1.41	2.15	0.00	0.00	FUT7
A_23_P86599	1.41	3.58	0.01	1.80E-05	DMBT1
A_23_P500501	1.39	2.69	0.00	5.00E-06	FGFR3
A_23_P251855	1.38	2.56	0.00	6.00E-06	SLC12A7
A_24_P404245	1.37	2.61	0.01	7.60E-05	PCYT2
A_23_P10391	1.36	0.79	0.00	0.00	COL5A2
A_23_P147331	1.36	1.3	0.00	0.00	SERINC2
A_24_P206305	1.35	2.95	0.02	8.80E-05	MICALL2
A_23_P356004	1.35	2.42	1.90E-05	0.00	KCNIP3
A_23_P73023	1.34	1.19	0.00	0.00	TBC1D1
A_24_P687305	1.33	1.79	0.02	0.00	DKFZp434K191
A_24_P123601	1.33	2.19	0.01	0.00	DDR1
A_23_P51187	1.32	3.01	0.05	0.00	PRKCZ
A_23_P128993	1.32	1.06	5.90E-05	6.90E-05	GZMH
A_23_P93311	1.31	2.2	0.00	7.80E-05	DDR1
A_24_P188116	1.31	2.19	0.01	0.00	ANKRD2
A_23_P101193	1.3	1.19	0.00	0.00	MYO5B
A_23_P76749	1.28	0.73	0.01	0.03	GALNTL1
A_24_P623768	1.28	0.79	0.01	0.03	AF131813
A_24_P290751	1.28	1.74	0.00	0.00	DTX1
A_24_P48898	1.27	1.37	0.04	0.01	APOL2
A_24_P346431	1.27	2.7	0.04	0.00	TNS3

Se-Ax cells were transfected as described in Fig. S3. Table of all genes that showed at least a log₂-fold change > 1.0 or < -1.0 and an adjusted p-value of P < 0.05 in the comparison E47-FD vs. Mock. According log₂-fold changes and adjusted p-values of the comparison E47 vs. Mock are also stated. Calculation of adjusted p-values was done as described in Fig. S3.

Table S5. E2A-regulated genes in Se-Ax cells (Continued)

Agilent probe ID	Log ₂ -fold change: E47-FD vs. Mock	Log ₂ -fold change: E47 vs. Mock	Adjusted p-value: E47-FD vs. Mock	Adjusted p-value: E47 vs. Mock	Gene symbol
A_32_P35947	1.27	4.31	0.00	1.00E-06	LOC651758
A_23_P259141	1.27	1.28	5.90E-05	1.80E-05	ZBP1
A_23_P22723	1.26	1.14	0.04	0.02	ATP2B3
A_23_P47614	1.26	2.48	0.01	0.00	PHLDA2
A_23_P68786	1.26	2.92	0.01	3.20E-05	PRODH
A_24_P693986	1.26	1.54	0.01	0.00	LOC388610
A_24_P406132	1.26	1.39	0.02	0.01	MAPK13
A_32_P17182	1.25	0.67	0.00	0.01	N48043
A_24_P50890	1.25	3.39	2.00E-04	0.00	PVRL1
A_23_P168449	1.24	2.58	0.05	0.00	RASA4
A_23_P14508	1.23	1.24	0.00	0.00	TTC9
A_23_P137381	1.22	1.37	0.04	0.01	ID3
A_23_P49546	1.22	2.93	0.00	1.00E-06	GRIN2C
A_23_P417415	1.22	1.02	0.00	0.00	ACOT11
A_23_P42882	1.21	4.26	0.00	0.00	CAMK2B
A_23_P52286	1.21	1.19	0.00	0.00	RP11-529110.4
A_24_P213503	1.2	2.2	0.00	5.00E-06	PTPRE
A_23_P161659	1.19	1.29	0.00	4.20E-05	SYT13
A_23_P165333	1.18	1.15	0.00	0.00	BIN1
A_23_P258088	1.17	0.79	0.00	0.00	PACSIN1
A_23_P53081	1.17	2.27	0.02	0.00	OSBPL5
A_23_P168388	1.16	1.25	0.01	0.00	GIMAP8
A_23_P95029	1.16	0.66	0.00	0.01	SNTB1
A_23_P354175	1.16	1.58	0.01	0.00	TMEM129
A_23_P213944	1.16	0.93	0.00	0.00	HBEGF
A_24_P677559	1.16	0.75	0.00	0.00	BC032451
A_23_P93641	1.15	1.71	0.02	0.00	AKR1B10
A_23_P54846	1.15	1.04	0.02	0.01	HERPUD1
A_23_P76538	1.14	1.9	0.00	6.30E-05	TESC
A_23_P431933	1.14	1.56	0.01	0.00	CAMKK1
A_23_P127781	1.13	1.68	0.01	0.00	SCGB1D1
A_23_P311912	1.13	3.7	0.01	4.00E-06	C14orf78
A_23_P145376	1.13	1.19	0.04	0.01	MAPK13
A_32_P149011	1.12	0.58	0.00	0.04	CN479126
A_23_P390984	1.12	2.38	0.02	0.00	KCNH6
A_23_P169137	1.12	1.48	0.00	6.60E-05	NINJ1
A_23_P502314	1.12	1.27	0.02	0.00	CD97
A_32_P5976	1.11	2.14	0.02	0.00	NUDT14
A_24_P91094	1.11	2.24	0.00	7.00E-06	RPIP8
A_23_P60990	1.11	3.69	0.00	1.00E-06	FLJ22671
A_24_P372913	1.11	1.63	0.00	1.50E-05	TCF1
A_23_P110569	1.1	1.43	0.03	0.00	TRIM36
A_23_P502312	1.1	1.16	0.01	0.00	CD97
A_24_P129341	1.1	1.64	0.00	0.00	AKR1B10
A_23_P123848	1.1	2.08	0.00	1.30E-05	DAB2IP
A_32_P201292	1.09	0.92	0.00	0.00	BU587941
A_24_P132383	1.09	1.25	0.00	0.00	GIMAP8
A_32_P9543	1.09	1.94	0.05	0.00	APOBEC3A
A_24_P83758	1.09	2.49	0.00	6.00E-06	ENST00000292728

Se-Ax cells were transfected as described in Fig. S3. Table of all genes that showed at least a log₂-fold change > 1.0 or < -1.0 and an adjusted p-value of P < 0.05 in the comparison E47-FD vs. Mock. According log₂-fold changes and adjusted p-values of the comparison E47 vs. Mock are also stated. Calculation of adjusted p-values was done as described in Fig. S3.

Table S5. E2A-regulated genes in Se-Ax cells (*Continued*)

Agilent probe ID	Log ₂ -fold change: E47-FD vs. Mock	Log ₂ -fold change: E47 vs. Mock	Adjusted p-value: E47-FD vs. Mock	Adjusted p-value: E47 vs. Mock	Gene symbol
A_24_P367289	1.08	1.8	0.01	0.00	DDR1
A_23_P76901	1.08	1.36	0.00	0.00	PLEKHG3
A_24_P156993	1.08	1.05	0.01	0.00	BIN1
A_23_P19894	1.07	0.91	0.01	0.01	AQP1
A_24_P152845	1.07	1.59	0.00	2.50E-05	LOC340888
A_23_P6746	1.07	1.99	0.01	4.80E-05	IQSEC1
A_23_P79978	1.05	0.84	0.05	0.04	SLC24A3
A_24_P145629	1.05	0.99	0.03	0.02	SERINC2
A_23_P67198	1.05	1.47	0.00	1.40E-05	CPAMD8
A_23_P157247	1.04	2.00	0.00	6.00E-06	MGC9712
A_23_P404667	1.04	2.36	0.03	0.00	BIK
A_23_P12463	1.04	0.79	0.00	0.00	QSCN6
A_23_P209799	1.03	1.58	0.00	0.00	MYO7B
A_23_P34537	1.03	1.62	0.02	0.00	EPHX1
A_23_P165840	1.03	1.32	0.01	0.00	ODC1
A_23_P214408	1.02	2.81	0.00	0.00	UNC93A
A_23_P395460	1.02	3.38	0.01	3.00E-06	KIF1A
A_23_P165927	1.02	3.72	0.01	1.00E-06	STMN3
A_24_P103434	1.01	2.92	0.00	0.00	UNC93A
A_23_P401076	1.01	1.64	0.04	0.00	SUSD3
A_23_P35092	-1.09	-1.13	0.02	0.01	IL19

Se-Ax cells were transfected as described in Fig. S3. Table of all genes that showed at least a log₂-fold change > 1.0 or < -1.0 and an adjusted p-value of P < 0.05 in the comparison E47-FD vs. Mock. According log₂-fold changes and adjusted p-values of the comparison E47 vs. Mock are also stated. Calculation of adjusted p-values was done as described in Fig. S3.

Table S6. Genes overlapping between our dataset and GSE4784, GSE4693, or GSE4784 and GSE4693

Overlap between our data and Schwartz et al. (GSE4784)	Overlap between our data and Ikawa et al. (GSE4693)	Overlap between our data and Schwartz et al. and Ikawa et al.
ALDH1L1	ADA	ATOH8
AMPD3	ADRA2C	BTG2
ATF3	AKR1B10	CAMK2B
ATOH8	ART3	CBFA2T3
AZI1	ATOH8	CDKN1A
BCL2L11	BIK	CHIT1
BDKRB2	BMF	CPNE5
BTG2	BTG2	DYSF
BZRAP1	CAMK2B	EDN2
C3orf54	CBFA2T3	GADD45B
CAMK2B	CCDC96	GPR56
CBFA2T3	CD82	HERPUD1
CCNL1	CDKN1A	HES1
CDKN1A	CHIT1	HTRA3
CDKN1C	CPNE5	ID2
CHIT1	CTSA	IGHM
CPEB4	CUZD1	KCNQ1
CPNE5	DTX1	PDGFA
CSRP1	DYSF	PTGDS
DLL1	EDN2	PTP4A3
DYSF	ENTPD8	SSTR2
EDN2	FES	SYNGR2
EPB41L4B	FGFR3	TCIRG1
FBLN2	GADD45B	XBP1
FGF9	GNAZ	ZDHHC8
GADD45B	GPR20	
GLCC11	GPR56	
GLDC	HERPUD1	
GPR56	HES1	
GRHL1	HTRA3	
GRIN2C	ID2	
HERPUD1	ID3	
HES1	IER5L	
HIVEP3	IFIH1	
HTRA3	IGHM	
ID1	IRF7	
ID2	KCNQ1	
IGHM	KLK1	
IGSF3	KLK10	
IL11RA	LFNG	
IL21R	LSP1	
ITGA6	LTB	
JAG2	MAL	
KCNJ12	MAP1LC3B	
KCNQ1	MARCO	
KLHL21	MGLL	
KRT17	MYO7A	
KRT5	NINJ1	
MAN2A1	NINJ2	
NOXO1	OXT	
NUAK2	PDGFA	

Table S6. Genes overlapping between our dataset and GSE4784, GSE4693, or GSE4784 and GSE4693 (*Continued*)

Overlap between our data and Schwartz et al. (GSE4784)	Overlap between our data and Ikawa et al. (GSE4693)	Overlap between our data and Schwartz et al. and Ikawa et al.
NUDT14	PHLDA2	
PDGFA	PKD1	
PRODH	PRAP1	
PRSS3	PRKCZ	
PTGDS	PTGDS	
PTP4A3	PTP4A3	
PTPRE	RASSF4	
PVRL1	RGR	
RASA4	RSAD2	
RASAL1	SERINC2	
RBM38	SGCA	
RGS16	SLC24A3	
SEMA3F	SLC04A1	
SFTPC	SNAI3	
SLC24A6	SPRR1A	
SPACA3	SPRR1B	
SPRR3	SSTR2	
SSTR2	STMN3	
SYNGR2	SYNGR2	
SYT12	TCIRG1	
TCIRG1	TESC	
TMEM129	TFPI	
TPST2	TGFB3	
XBP1	TGM2	
ZDHHC8	TNFRSF25	
ZNF238	TNNT2	
	TUBB3	
	WNT10A	
	WNT4	
	WNT5B	
	XBP1	
	ZBP1	
	ZDHHC8	
	ZG16	

Shown are all gene symbols, which in either dataset comparison are up-regulated at least 1.5-fold in the datasets used for the respective comparison.

Table S7. Sequencing results of *E2A* coding regions

Patient no.	SNPs and mutations detected in coding region	Type	Zygoty
4	rs1140828	synonymous	heterozygous
	rs1052692	non synonymous	heterozygous
	rs1052696	synonymous	heterozygous
	rs8140	synonymous	heterozygous
5	none	-	-
6	none	-	-
7	rs1140828	synonymous	homozygous
	rs1052692	non synonymous	heterozygous
	rs1052696	synonymous	heterozygous
	rs8140	synonymous	homozygous
10	rs1140828	synonymous	heterozygous
	rs1052692	non synonymous	heterozygous
	rs1052696	synonymous	heterozygous
	rs8140	synonymous	heterozygous
11	rs1140828	synonymous	homozygous
	rs8140	synonymous	homozygous
12	none	-	-
13	none	-	-
15	rs8140	synonymous	homozygous
	rs2074888	non synonymous	homozygous
16	Mutation (G → A; 1572856)	synonymous	heterozygous
	rs1140828	synonymous	heterozygous
	rs8140	synonymous	heterozygous
17	rs1140828	synonymous	homozygous
	rs8140	synonymous	homozygous
19	rs1140828	synonymous	homozygous
	rs1052692	non synonymous	heterozygous
	rs1052696	synonymous	heterozygous
	rs8140	synonymous	homozygous
20	rs1140828	synonymous	homozygous
	rs8140	synonymous	homozygous

Shown are all detected single nucleotide polymorphisms (SNPs) and yet undescribed alterations (mutations) within the coding regions of *E12* as well as *E47* in enriched tumor cells from SS patients. For the detected mutation the altered base and its position according to HG18 is given in brackets.

Table S8. Array platforms used in this study

Patient no.	Array platform		
1	BAC	400k	-
2	BAC	-	60k
3	BAC	400k	-
4	BAC	-	60k
5	BAC	400k	-
6	BAC	400k	-
7	BAC	-	60k
8	BAC	400k	-
9	BAC	-	-
10	BAC	-	-
11	BAC	400k	-
12	BAC	400k	-
13	BAC	400k	-
14	BAC	-	-
15	-	400k	-
16	BAC	400k	-
17	BAC	400k	-
18	BAC	400k	-
19	BAC	400k	-
20	BAC	400k	-
Se-Ax	BAC	-	-

Experiments in bold type were used for defining the genomic coordinates of DNA copy number changes visualized in Fig. 1 A, Fig. S1, and Table S2. BAC, 36k whole-genome tiling path BAC array. 400k, 400k whole-genome oligonucleotide array. 60k, custom 60k chromosome 19p oligonucleotide array.

REFERENCES

- Ikawa, T., H. Kawamoto, A.W. Goldrath, and C. Murre. 2006. E proteins and Notch signaling cooperate to promote T cell lineage specification and commitment. *J. Exp. Med.* 203:1329–1342. doi:10.1084/jem.20060268
- Schwartz, R., I. Engel, M. Fallahi-Sichani, H.T. Petrie, and C. Murre. 2006. Gene expression patterns define novel roles for E47 in cell cycle progression, cytokine-mediated signaling, and T lineage development. *Proc. Natl. Acad. Sci. USA.* 103:9976–9981. doi:10.1073/pnas.0603728103